MODELLING AND ANALYSIS OF A DELAY INDUCED DYNAMICAL MODEL ON ONCOLYTIC VIROTHERAPY WITH TUMOR EXTINCTING OPTIMAL STRATEGIES

Hitesh Kumar Singh, Dwijendra Narain Pandey, Mahendra
Department of Mathematics, Indian Institute of Technology, Roorkee
Roorkee-247667, India
Emails: hksinghiitr@gmail.com, dwij.iitk@gmail.com, mahi.070794@gmail.com

Abstract. In this paper, we study a non-linear delayed dynamical model that illustrates the interaction between an oncolytic virus and the cancerous cells. The model includes two kind of cancerous cells, infected ones (infected by an oncolytic virus) and uninfected ones. The necessary stability conditions are established in order to stabilize the system in equilibrium. The burst size of the virus has a critical value below which the therapy fails and beyond which the partial success of the therapy takes place. The inclusion of the delay in the model leads to periodic solutions. Further, we include two controls, one to optimize rate of infection and other to optimize viral load. The corresponding three strategies are discussed and concluded that combination of first two strategies comes out to be best in extinction of the tumor completely. Numerical simulations are done using MATLAB software. We have used forward-backward sweep method to simulate the optimal control problem.

1. Introduction

Today cancer is one of the major life-threatening disease worldwide. Also, it is going to be an increasingly requisite cause of death worldwide in the coming decades. The International Agency for Research on Cancer (IARC) has estimated that even if the current cancer rates does not alter, the estimated new cases of cancer will rise to 22 million by 2030 [1]. Also, it is predicted by IARC that almost half of the total affected population lives in medium and low-income countries [2]).

Treatments for cancer involve surgery, chemotherapy, radiotherapy etc. But usually, the patients know about the disease when they left with very less options for therapy. Some tumors, being completely chimerical, require a wide range of therapeutic strategies. Oncolytic virotherapy is one of the most promising treatments of cancer that is being developed over the past few decades. Oncolytic virotherapy is a kind of cancer treatment that uses the oncolytic virus replication inside the tumor to destroy cancerous cells keeping all other noncancerous cells unharmed. Oncolytic viruses are of two kinds; one that occur naturally in human cancer cells and other that are engineered by modifying the gene in order to achieve an optimal outcome. There are several genetic methods and several genetically modified oncolytic viruses [3]. Herpesviruses, adenoviruses, measles viruses, Coxsackieviruses, etc. are few instances of oncolytic viruses [4]. H101 was the first genetically modified oncolytic virus made by 'Shanghai Sunway Biotech' which, in 2005, got approval from the Chinese State Food and Drug Administration (SFDA) in order to cure neck and head cancer [5, 6]. An adenovirus, ONYX-015, has drawn up a large attention because it has been proven to be pretty much effective in decaying the tumor load and removing it [7]. ONYX-015, engineered in 1987, infects the cancerous cells selectively and kill them by making a defect in their p53 gene [8, 9].

Mathematical modelling of the interaction between virus and cell is being done since more than 20 years back [10–12]. Particularly in HIV infection, e.g., Ho et al. [13] and Wei et al. [14], the interaction between HIV virus and $CD4^+$ T-cells has been successfully modelled mathematically which encourages mathematicians and biologists to work with the same scenario here in oncology. Oncolytic virotherapy also involves the interaction between the replicating virus and emerging tumor that requires to be modelled

Key words and phrases. Tumor, Oncolytic virus, Delay, Stability, Bifurcation, Optimal control.
Mathematics Subject Classification 2020: 34C23, 34D20, 37N25, 49J15, 92B05.

2 Jul 2023 07:17:33 PDT
230319-Singh Version 2 - Submitted to Rocky Mountain J. Math.

mathematically. These mathematical models of virus-host interaction predict the possible results of viral-infection and govern the optimal virotherapy. However, results proven in clinical trials suggest that the infection of the oncolytic virus on tumor cells may have no clear effect to stabilization or removal of tumor [15].

Several models have been introduced so far in this regard. Initially, the mathematical models of oncolytic virotherapy involving ordinary differential equations illustrating the interaction between virus-infected cancerous cells and non-infected cancerous cells were introduced. Later on, because of possessing different spatial structures, these ODE models required a necessary extension to PDE models [16]. In 2005, Tao et al. [17] extended the model proposed by Wein et al. [18] and showed the global existence of the solution along with uniqueness.

A variety of functional responses also have been suggested in different works by many authors [19–22]. The prey dependent functional response, also known as mass-action law in chemical kinetics has been introduced in Lotka and Volterra equations. It is taken in many papers e.g. [20, 23, 24] etc. In 1959, Holling introduced a new type of functional response that takes the saturation effect into account [25]. In 1989, Arditi and Ginzberg [19] proposed a more realistic functional response known as ratio dependent functional response which is both prey dependent and predator dependent as well. In 2005, A. S. Novozhilov et al. [22] and in 2003, Hwang et al. [21] etc. used the ratio dependent functional response in their manuscripts.

It is obvious that not all real phenomena are instantaneous and in completing the task some time is lagged. This time lag induces a delay in the dynamical systems. This delay can be the delay of immune system to respond [26], the delay of maturation [27], the delay of gestation period [28], etc. Several authors have studied the dynamical systems of prey-predator models and SIR models including delays [29–34]. Several monographs have been written regarding the delay induced dynamical systems [35–37].

Furthermore, in order to minimize or extinct a disease infection in a community or in a species' organ, the theory of optimal control provides a strong mechanism. Many authors have constructed mathematical models investigating the disease transmission and their control [38–40]. Our goal, in this paper, is to minimize the tumor volume using firstly a delay dynamical system on oncolytic virotherapy and then the same problem with optimal controls. We discuss three different optimal strategies regarding this and compare all three optimal strategies for tumor reduction and elimination.

Definition: Let $C([-\tau, 0], \mathbb{R})$, denoted by $\mathcal{C}$, be a Banach space of all the continuous functions from the closed interval $[-\tau, 0]$ to $\mathbb{R}$ equipped with the sup norm $||f(x)||_\infty = \sup_{a \le x \le b} |f(x)| \ \forall \ f \in \mathcal{C}$. The non-negative cone of $\mathcal{C}$ is denoted by $\mathcal{C}^+ = C([-\tau, 0], \mathbb{R}^+ \cup \{0\})$.

Comparison theorem(used in theorem 3.2 in this paper in order to prove boundedness of the solution): Suppose $x(t)$ and $y(t)$ are continuous functions defined on the interval $[a, b]$ of the real line $\mathbb{R}$ and differentiable on $(a, b]$. Let f be a continuous function from $\mathbb{R} \times \mathbb{R}$ to $\mathbb{R}$. Then $x < y$ if

$$x(a) < y(a) \ and \ \frac{dx}{dt} - f(t, x(t)) < \frac{dy}{dt} - f(t, y(t)) \ in \ (a, b].$$

This paper is structured as follows. The delay model is formulated in Section 2. Section 3 consists of positivity and boundedness of the solutions of the model. The stability analysis of the model is done in Section 4. Section 5 is consisting of numerical simulations of the delay model without optimal control. Section 6 contains the formulation of the delayed optimal control problem. The penultimate section includes numerical simulations of the control problem and the final section contains discussion and conclusions.

2. The Model

Delay in the dynamical systems always causes analytical complexity but makes the problem more realistic in nature. Presence of the delay, sometimes, may affect the system so much that nice looking phase portraits may change to periodic solutions or even chaos. This motivates us to introduce a delay in the model proposed in [24], that shows the interaction between infected tumor cells, uninfected tumor cells that are susceptible to be infected and the virus. The uninfected cells when come into the contact

of free virus particles, they do not become infected instantaneously and some time is required for them to become actively infected. Incorporating this delay, the model takes the form,

$$\begin{aligned}\frac{dU}{dt} &= rU\left(1-\frac{U+I}{K}\right)-\alpha UI-\beta UV\\ \frac{dI}{dt} &= \beta U(t-\tau)V(t-\tau)-\gamma I\\ \frac{dV}{dt} &= b\gamma I-\delta V-\beta UV.\end{aligned} \tag{2.1}$$

subjected to the initial history $U(t)=\phi_u(s)\geq 0$, $I(t)=I(0)=I_0\geq 0$ and $V(t)=\phi_v(s)\geq 0\ \forall\ t\in[-\tau,0]$. Here U, I and V are the sizes of uninfected cells, infected cells, and free virus population respectively, r is the growth rate of uninfected cell population, K is the maximal tumor size, α is the rate by which fusion of uninfected and infected cells takes place resulting in a syncytium [41], β is the rate of infection, γ is the rate by which infected cells are dying, δ is the rate of elimination of free virus particles and b represents the number of new virus particles which are released by an infected cell while rupturing. The natural death rate of the uninfected cells can be neglected without affecting the phase portraits of the system [22]. All these parameters are supposed to be positive. It is also assumed that infected tumor cell can not be divided further into two new cells. The functional response is considered as prey dependent.

3. Positivity and Boundedness of the Solutions

Lemma 3.1. *Starting with the initial condition $(\phi_u(s),I_0,\phi_v(s))\in\mathcal{C}^+\times\mathcal{R}^+\times\mathcal{C}^+\ \forall\ s\in[-\tau,0]$, the system (2.1) has a unique solution. Moreover, this solution remains non-negative for all $t\geq 0$.*

Proof. Using the fundamental theory of functional differential equations [42], the existence of unique local solution is confirmed. Now, integrating the first equation of the system (2.1), we get

$$U(t)=\phi_u(0)e^{\int_0^t[r(1-\frac{U(s)+I(s)}{K})-\alpha I(s)-\beta V(s)]ds}.$$

Using the non-negativity of the initial condition and the exponential function, we get that $U(t)\geq 0\ \forall\ t\geq 0$.
Integrating the second equation of the system (2.1),

$$I(t)e^{\gamma t}-I_0=\beta\int_0^t e^{\gamma s}U(s-\tau)V(s-\tau)ds.$$

It implies that when $0\leq t\leq\tau$,

$$I(t)=e^{-\gamma t}[I_0+\beta\int_0^t e^{\gamma s}\phi_u(s-\tau)\phi_v(s-\tau)ds]. \tag{3.1}$$

Since $(\phi_u(s),I_0,\phi_v(s))\in\mathcal{C}^+\times\mathcal{R}^+\times\mathcal{C}^+$ and $e^{-\gamma t}>0$, we have $I(t)\geq 0\ \forall\ t\in[0,\tau]$.
Now integrating the third equation of the system (2.1) from 0 to t, we get

$$V(t)e^{\int_0^t(\delta+\beta U(s))ds}-\phi_v(0)=b\gamma\int_0^t e^{\int_0^s(\delta+\beta U(x))dx}I(s)ds,$$

when $0\leq t\leq\tau$,

$$V(t)=e^{-\int_0^t(\delta+\beta U(s))ds}[\phi_v(0)+b\gamma\int_0^t e^{\int_0^s(\delta+\beta U(x))dx}I(s)ds]. \tag{3.2}$$

Again, using the non negativity of the initial condition and the exponential function, we have $V(t)\geq 0$ $\forall\ t\in[0,\tau]$.
Now, using the non negativity of the functions $I(t)$ and $V(t)$ in the interval $[0,\tau]$, we can show that $I(t)$ and $V(t)$ are non negative in $[\tau,2\tau]$. Repeating the same process infinitely many times, we have that $I(t)$ and $V(t)$ are non negative for all $t\geq 0$. □

Theorem 3.2. *Starting with the non negative initial conditions* $U(s) = \phi_u(s) \leq K$, $I(0) = I_0 \leq \frac{rK}{\mu}$; $\mu \leq \min\{r, \gamma\}$ *and* $V(s) = \phi_v(s) \leq \frac{b\gamma rK}{\mu\delta}$; $s \in [-\tau, 0]$, *any solution of the system (2.1) is uniformly bounded.*

Proof. (i) We have

$$\frac{dU}{dt} = rU(t)\left(1 - \frac{U(t) + I(t)}{K}\right) - \alpha U(t)I(t) - \beta U(t)V(t).$$

Since $U(t)$, $I(t)$ and $V(t) \geq 0 \ \forall \ t > 0$, we have

$$\frac{dU}{dt} \leq \frac{rU(t)}{K}(K - U(t)).$$

Now, using the comparison theorem, we have

$$U(t) \leq K \ \forall \ t \geq 0.$$

and hence $\limsup_{t\to\infty} U(t) \leq K$.
(ii) From the first two equations of the system (2.1), we have

$$\begin{aligned} U'(t) + I'(t+\tau) &= rU(t)(1 - \frac{U(t) + I(t)}{K}) - \alpha U(t)I(t) - \gamma I(t+\tau), \\ &\leq r(K - U(t)) - \gamma I(t+\tau) \end{aligned}$$

assuming $\mu = \min\{r, \gamma\}$, we get

$$(U(t) + I(t+\tau))' = rK - \mu(U(t) + I(t+\tau)),$$

thus we obtain $U(t) + I(t+\tau) \leq \frac{rK}{\mu}$ and hence $\limsup_{t\to\infty}(U(t) + I(t+\tau)) \leq \frac{rK}{\mu}$. Now, since $U(t) \geq 0$, we have $\limsup_{t\to\infty} I(t+\tau) \leq \frac{rK}{\mu}$ and hence $\limsup_{t\to\infty} I(t) \leq \frac{rK}{\mu}$.
(iii) Since $U(t)$ and $V(t)$ are positive for all $t > 0$, from the third equation of the system (2.1), we have

$$\begin{aligned} V'(t) &\leq b\gamma I - \delta V, \\ &\leq \frac{b\gamma rK}{\mu} - \delta V. \end{aligned}$$

Thus, using comparison theorem, we obtain $V(t) \leq \frac{b\gamma rK}{\mu\delta}$ and hence $\limsup_{t\to\infty} V(t) \leq \frac{b\gamma rK}{\mu\delta}$.

□

Now, we can analyze the dynamics of the system (2.1) in the following positively invariant bounded feasible region $\mathfrak{M}$ defined as

$$\mathfrak{M} = \{(U, I, V) \in \mathcal{C}^+ \times \mathcal{R}^+ \times \mathcal{C}^+ : ||U|| \leq K, ||U + I|| \leq \frac{rK}{\mu}, ||V|| \leq \frac{b\gamma rK}{\mu\delta}\}$$

4. Stability Analysis

The points of equilibrium of the system (2.1) are

(1) $E_1(0, 0, 0)$,
(2) $E_2(K, 0, 0)$, and
(3) $E_3\left(\frac{\delta}{\beta(b-1)}, \frac{\delta r(Kb\beta - \delta - K\beta)}{\beta(b-1)(\delta r - K\gamma\beta + K\delta\alpha + Kb\gamma\beta)}, \frac{\gamma r(Kb\beta - \delta - K\beta)}{\beta(\delta r - K\gamma\beta + K\delta\alpha + Kb\gamma\beta)}\right)$.

The value of burst size b can not be less than 1 because if so, virus particles will vanish and then in this situation, tumor can not undergo any kind of virus infection and virotherapy fails.
For any equilibrium solution (U^*, I^*, V^*), the corresponding linearized system is

$$\frac{dX}{dt} = AX(t) + BX(t-\tau) \tag{4.1}$$

$$A = \begin{pmatrix} r(1 - \frac{2U^* + I^*}{K}) - \alpha I^* - \beta V^* & -r\frac{U^*}{K} - \alpha U^* & -\beta U^* \\ 0 & -\gamma & 0 \\ -\beta V^* & b\gamma & -\delta - \beta U^* \end{pmatrix},$$

$$B = \begin{pmatrix} 0 & 0 & 0 \\ \beta V^* & 0 & \beta U^* \\ 0 & 0 & 0 \end{pmatrix}.$$

4.1. **Instability of The Trivial Steady State E_1.**

Theorem 4.1. *The origin is always an unstable saddle point and independent of delay values.*

Proof. At $E_1(0,0,0)$,

$$A = \begin{pmatrix} r & 0 & 0 \\ 0 & -\gamma & 0 \\ 0 & b\gamma & -\delta \end{pmatrix},$$

and B is the null matrix. Thus the characteristic equation is given by

$$\begin{aligned} \det(\lambda I - A) &= 0, \\ (\lambda - r)(\lambda + \gamma)(\lambda + \delta) &= 0. \end{aligned} \tag{4.2}$$

Which is a cubic polynomial in λ having one positive root r and two negative roots $-\gamma$ and $-\delta$. So, the equilibrium point $(0,0,0)$ is always an unstable saddle due to the presence of opposite sign real roots. □

4.2. **Local Asymptotic Stability of The Therapy Failure Steady State E_2.**

Theorem 4.2. *If $b \leq 1 + \frac{\delta}{\beta K}$, then the equilibrium point $(K,0,0)$ is always a locally asymptotically stable and unstable if $b > 1 + \frac{\delta}{\beta K}$, i.e., transcritical bifurcation exists at $b = 1 + \frac{\delta}{\beta K}$ as a point of bifurcation.*

Proof. The proof of the same can be seen in [43]. □

4.3. **Global Asymptotic Stability of The Therapy Failure Steady State E_2.**

Theorem 4.3. *The equilibrium point E_2, i.e., $(K,0,0)$ is globally asymptotically stable in $\mathfrak{M}$ if $b < 1 + \frac{\delta}{\beta K}$.*

Proof. Constructing a Lyapunov functional $L : \mathcal{C} \times \mathcal{R} \times \mathcal{C} \to \mathcal{R}$ on domain $\mathfrak{M}$ defined as

$$L(U,I,V) = bI(t) + V(t) + b\beta \int_{t-\tau}^{t} U(\theta)V(\theta)d\theta,$$

Clearly, L is positive definite in $\mathfrak{M}$.
Calculating the derivative of L with respect to time t along the solutions of system (2.1), we get

$$\dot{L}|_{(2.1)} = b\dot{I}(t) + \dot{V}(t) + b\beta \frac{d}{dt} \int_{t-\tau}^{t} U(\theta)V(\theta)d\theta,$$

applying Leibniz integral rule, we obtain

$$\dot{L}|_{(2.1)} = b\dot{I}(t) + \dot{V}(t) + b\beta U(t)V(t) - b\beta U(t-\tau)V(t-\tau).$$

Using the values of $\dot{I}(t)$ and $\dot{V}(t)$ from system (2.1), we get

$$\begin{aligned} \dot{L}|_{(2.1)} &= b\beta U(t)V(t) - \beta U(t)V(t) - \delta V(t), \\ &= V(t)[\beta U(t)(b-1) - \delta], . \end{aligned}$$

But, $U(t) \leq K$ in the region $\mathfrak{M}$, Thus, we get

$$\dot{L}|_{(2.1)} \leq V(t)[\beta K(b-1) - \delta].$$

Clearly, if $b < 1 + \frac{\delta}{\beta K}$, then $\dot{L} \leq 0$ and for each $t \geq 0$, $\dot{L} = 0$ if and only if $V(t) = 0$. Now, let M be the largest invariant set in the set $E = \{(U,I,V) | \dot{L} = 0\}$. From the system of equations (2.1) and the invariance of $\mathfrak{M}$, we get that $M = \{(K,0,0)\}$. It follows from the Lyapunov Lasalle invariance principle [44] that $(K,0,0)$ is globally asymptotically stable when $b < 1 + \frac{\delta}{\beta K}$. □

4.4. **Stability of The Steady State E_3.** Now, the positive equilibrium point E_3 exists if

$$b > 1 + \frac{\delta}{\beta K} \tag{H1}$$

Furthermore, the characteristic equation for the positive steady state (U^*, I^*, V^*), using the matrices related to the differential equation (4.1), becomes

$$[\lambda - r\left(1 - \frac{2U^* + I^*}{K}\right) + \alpha I^* + \beta V^*][\lambda^2 + \lambda(\delta + \gamma + \beta U^*) + \gamma(\delta + \beta U^*) - b\beta\gamma U^* e^{-\tau\lambda}] + \beta V^* e^{-\tau\lambda}$$

$$[\lambda U^*\left(\alpha + \frac{r}{K}\right) + U^*\left(\alpha + \frac{r}{K}\right)(\delta + \beta U^*) + b\beta\gamma U^*] + \beta V^*[-\beta(U^*)^2\left(\alpha + \frac{r}{K}\right)e^{-\tau\lambda} - \beta U^*\lambda - \beta\gamma U^*)] = 0$$

which can be put into the form

$$(\lambda^3 + A_2\lambda^2 + A_1\lambda + A_0) + e^{-\tau\lambda}(B_1\lambda + B_0) = 0 \tag{4.3}$$

where $\tilde{t} = 1 - \frac{2U^*+I^*}{K}$,
$A_0 = (\alpha I^* - r\tilde{t})(\delta + \beta U^*)\gamma + \beta\gamma\delta V^*$,
$A_1 = (\delta + \gamma)(-r\tilde{t} + \alpha I^* + \beta V^*) + \beta U^*(-r\tilde{t} + \alpha I^*) + \gamma\delta + \beta\gamma U^*$,
$A_2 = \alpha I^* - r\tilde{t} + \beta(U^* + V^*) + \gamma + \delta$,
$B_0 = \beta\delta U^* V^*(\alpha + \frac{r}{K}) - b\beta\gamma U^*(-r\tilde{t} + \alpha I^*)$, and
$B_1 = -b\beta\gamma U^* + \beta U^* V^*(\alpha + \frac{r}{K})$.
For $\tau = 0$, assuming $C_0 = A_0 + B_0$ and $C_1 = A_1 + B_1$, we obtain

$$\lambda^3 + A_2\lambda^2 + C_1\lambda + C_0 = 0.$$

Now,

$$\begin{aligned}
C_0 &= A_0 + B_0, \\
&= (\alpha I^* - r\tilde{t})(\delta + \beta U^*)\gamma + \beta\gamma\delta V^* + \beta\delta U^* V^*(\alpha + \frac{r}{K}) - b\beta\gamma U^*(-r\tilde{t} + \alpha I^*), \\
&= (\alpha I^* - r\tilde{t})\gamma\delta + (1-b)(\alpha\beta\gamma U^* I^* - \beta\gamma r\tilde{t} U^*) + \beta\delta V^*[\gamma + U^*(\alpha + \frac{r}{K})], \\
&= (\alpha I^* - r\tilde{t})[\gamma\delta + (1-b)\beta\gamma U^*] + \beta\delta V^*[\gamma + U^*(\alpha + \frac{r}{K})], \\
&> 0 \ at \ E_3.
\end{aligned}$$

Therefore, by Routh-Hurwitz criterion, E_3 is asymptotically stable if

$$A_2 > 0 \text{ and } A_2 C_1 > C_0. \tag{H2}$$

Now, suppose $\tau > 0$, then stability can be lost if and only if $\lambda(\tau)$ becomes purely imaginary. Therefore, putting $\lambda = \iota\omega$ in (4.3) and then separating real and imaginary parts, ω must satisfy

$$\cos(\tau\omega) = \frac{B_1\omega^2(\omega^2 - A_1) + B_0(\omega^2 A_2 - A_0)}{B_0^2 + B_1^2\omega^2} \tag{4.4}$$

$$\sin(\tau\omega) = \frac{B_1\omega(\omega^2 A_2 - A_0) - B_0\omega(\omega^2 - A_1)}{B_0^2 + B_1^2\omega^2} \tag{4.5}$$

squaring and adding equations (4.4) and (4.5), ω must be a root of the equation

$$\omega^6 + (A_2^2 - 2A_1)\omega^4 + (A_1^2 - B_1^2 - 2A_0A_2)\omega^2 + A_0^2 - B_0^2 = 0, \tag{4.6}$$

Let $\omega = \sqrt{\xi}$, then

$$p(\xi) = \xi^3 + (A_2^2 - 2A_1)\xi^2 + (A_1^2 - B_1^2 - 2A_0A_2)\xi + A_0^2 - B_0^2.$$

Clearly, the assumption

$$A_0 < B_0 \tag{H3}$$

confirms a positive root of p and hence of equation (4.6).
Now, the unique value of $\tau\omega \in [0, 2\pi]$ obtained from equations (4.4) and (4.5) is

$$\tau\omega = \cos^{-1}\left(\frac{B_1\omega^2(\omega^2 - A_1) + B_0(\omega^2 A_2 - A_0)}{B_0^2 + B_1^2\omega^2}\right)$$

if $\sin\tau\omega > 0, i.e., B_1\omega(\omega^2 A_2 - A_0) - B_0\omega(\omega^2 - A_1) > 0$ and

$$\tau\omega = 2\pi - \cos^{-1}\left(\frac{B_1\omega^2(\omega^2 - A_1) + B_0(\omega^2 A_2 - A_0)}{B_0^2 + B_1^2\omega^2}\right)$$

if $B_1\omega(\omega^2 A_2 - A_0) - B_0\omega(\omega^2 - A_1) \leq 0$.
Now, defining two sequences τ_j^1 and τ_j^2 for $j \in \mathbb{N}$, as

$$\tau_j^1 = \frac{1}{\omega}[\cos^{-1}\left(\frac{B_1\omega^2(\omega^2 - A_1) + B_0(\omega^2 A_2 - A_0)}{B_0^2 + B_1^2\omega^2}\right) + 2j\pi]$$

and

$$\tau_j^2 = \frac{1}{\omega}[2\pi - \cos^{-1}\left(\frac{B_1\omega^2(\omega^2 - A_1) + B_0(\omega^2 A_2 - A_0)}{B_0^2 + B_1^2\omega^2}\right) + 2j\pi]$$

On the basis of the above analysis, we, now, state a lemma and then a theorem.

Lemma 4.4. *Let ω be the root associated with $\tau^* \in \{\tau_j^1, \tau_j^2\}$; $j \in \mathbb{N}$. Then sign* $\left[\frac{d}{d\tau}Real(\lambda)\right]\Big|_{\tau=\tau^*} = sign\{p'(\omega^2)\}$.

Proof. Proof of this lemma can be seen in [43]. □

Theorem 4.5. *[43] Assume that the conditions (H1), (H2) and (H3) hold good. Let τ^* is defined as* $\min\{\tau_j^1, \tau_j^2\}$; $j = 1, 2, 3, 4, \ldots$. *Then the positive steady state E_3 is asymptotically stable (locally) when $\tau < \tau^*$ and at $\tau = \tau^*$, Hopf bifurcation occurs if and only if $p'(\omega^2) > 0$.*

Proof. Lemma 4.4 and the property of derivative of the real part of λ at τ^* directly imply the result. □

4.5. **Direction and Stability of Hopf Bifurcation.** For the direction and stability of Hopf bifurcation we have the following theorem.

Theorem 4.6. *The direction of Hopf bifurcation is governed by μ_2. The periodic solution is supercritical (subcritical) if $\mu_2 > 0$ ($\mu_2 < 0$); β_2 determines the stability of bifurcating periodic solutions as the solutions are orbitally stable (unstable) if $\beta_2 < 0$ ($\beta_2 > 0$); and T_2 determines the period of the bifurcating periodic solutions as the period decreases (increases) if $T_2 < 0$ ($T_2 > 0$).*

Proof. The proof of the theorem is given in Appendix. □

5. Numerical Simulation

In this section, the analytical results given in the above sections will be verified by depicting some time-series plots and phase portraits. Here, we assume that $1mm^3$ tumor volume consists of 10^6 cells [24]. The parameters are taken as given in the following table 1:

The data is taken from the paper [20]. For plotting the graphs, we have used "ode45" and "dde23" MATLAB solvers. In the Figure-1, we have chosen $\beta = 0.1$, $b = 1.1$ and rest of all the parameters are as shown in the tale Table1, then $1.1 = b < 1 + \frac{\delta}{\beta K} = 1.2$. It is clear from the figure that for any values of delay ($\tau = 0$, 0.5 or 1) and initial concentrations $(U_0, I_0, V_0) = (2, 1, 2)$, $(2, 3, 2)$ or $(2, 5, 2)$, the tumor attains its maximum value 10 mm^3 implying the global stability of the therapy-failure equilibrium point $(10, 0, 0)$ that virotherapy fails completely. In Figure-2, we have taken $\beta = 0.2$ and $b = 1.7$, then $1.7 = b > 1 + \frac{\delta}{\beta K} = 1.1$. In this case, the positive equilibrium point becomes stable. It is shown for three different delay values $\tau = 0$, 1 and 1.9. But as delay τ attains its critical value $\tau^* = 2$ *days*, periodic solutions occur and cells in the tumor oscillate between a certain minimum and maximum value leading to the appearance of stable limit cycle as shown in the phase portraits in Figure-3. This confirms the

TABLE 1. Parameters and their values

Parameters	Values
Uninfected cell reproductive rate (r)	0.45 day^{-1}
Carrying capacity (K)	10 mm^3
Fusion rate of uninfected cell and infected cell (α)	0.3 mm^{-3} day^{-1}
Rate of infection (β)	assumed
Mortality rate of infected cells (γ)	0.5 day^{-1}
Rate of elimination of virus particles (δ)	0.2 day^{-1}
Burst rate of virus particles (b)	assumed
Delay (τ)	$\in [0, 2]$ days
Initial concentration of uninfected cells (U_0)	3×10^6 cells
Initial concentration of infected cells (I_0)	2×10^6 cells
Initial concentration of free virus particles (V_0)	2×10^6 cells

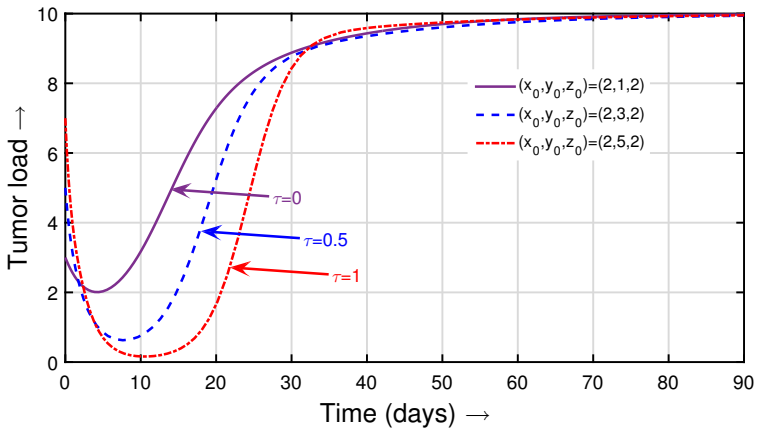

FIGURE 1. Global stability of the equilibrium point $(10, 0, 0)$ for different initial conditions and different delay values.

existence of Hopf bifurcation. Figure-4 and Figure-5 show the bifurcation diagrams for the parameters β and τ. Figures respectively show the critical values $\beta^* = 0.28$ and $\tau^* = 2$.

For the direction and stability of Hopf bifurcation, we have used the same set of parameter values as in Figure-3 and obtain $c_1(0) = -0.4315 + 0.1676i$. $\mu_2 = 173.1625 > 0$ implying that Hopf bifurcation is supercritical, $\beta_2 = -0.8631 < 0$ implying that the bifurcating periodic solution is orbitally asymptotically stable when $\tau > \tau^*$ (Figure-2 and Figure-3) and the period of bifurcating periodic solution is $T_2 = 0.3271 > 0$.

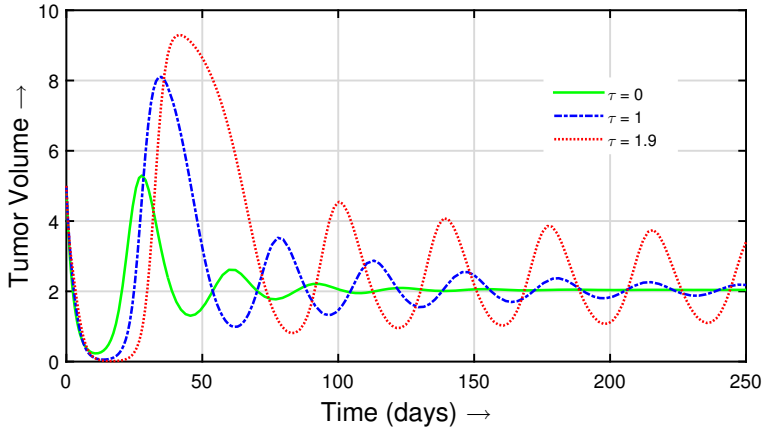

FIGURE 2. Impact of increasing values of infectivity delay τ over tumor load

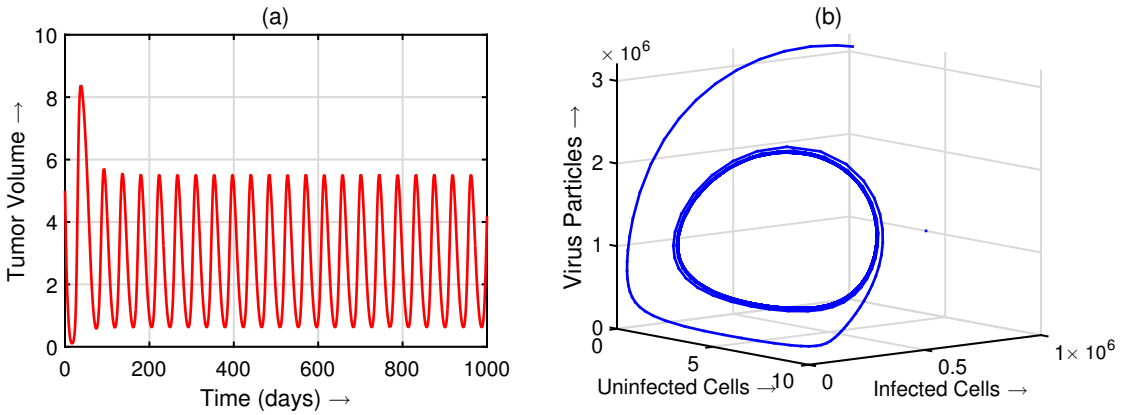

FIGURE 3. Appearance of limit cycle at $\tau = 2$

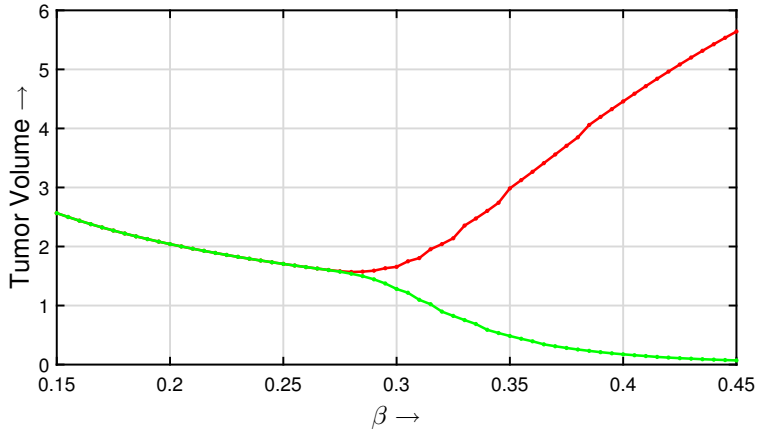

FIGURE 4. Bifurcation diagram for infection rate β.

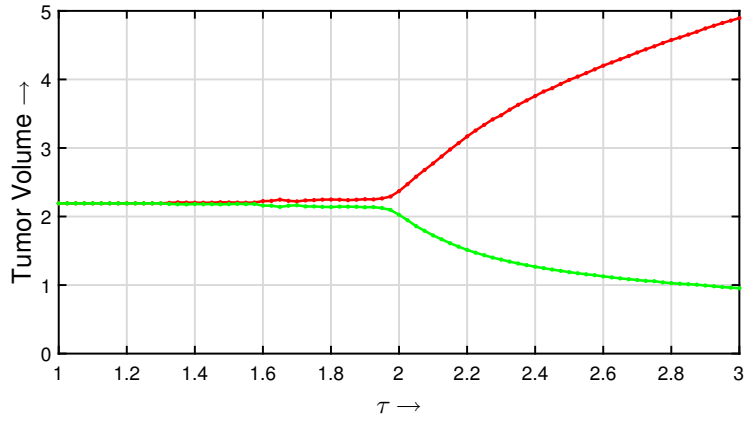

FIGURE 5. Bifurcation diagram for delay values τ.

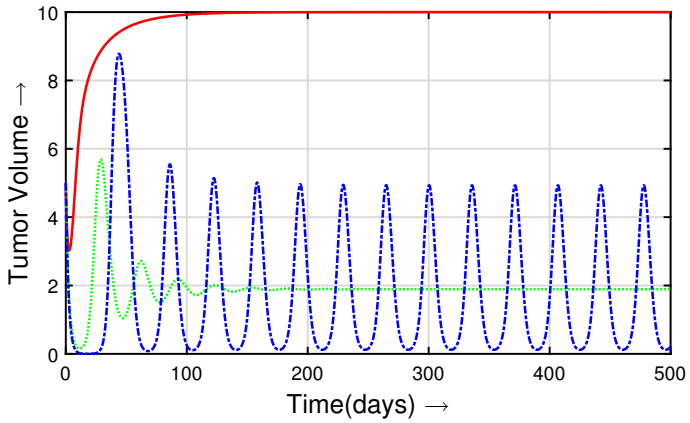

FIGURE 6. Tumor volume for different values of β; Red solid line for $\beta = 0.02$ $mm^{-3}day^{-1}$, green dotted line for $\beta = 0.22$ $mm^{-3}day^{-1}$ and blue dash-dot line for $\beta = 0.42$ $mm^{-3}day^{-1}$.

6. Optimal Control Problem

In this section, we will formulate an optimal control system based on the following control policies.

(i) Optimizing the rate of infection: Observing the Figure-4 and Figure-6, we conclude that β, the infection rate, is a sensitive parameter for the tumor growth, its stabilization and reduction. For the non delay system, if $\beta = 0.02$ mm^{-3} day^{-1}, tumor grows up to its maximal capacity 10 mm^3, if $\beta = 0.22$ mm^{-3} day^{-1}, tumor stabilizes to a certain value 1.9 mm^3 and if $\beta = 0.42$ mm^{-3} day^{-1}, tumor destabilizes again. This sensitivity of β motivates us to introduce an optimal control $u_1(t)$ in order to optimize the rate of infection β.

(ii) Optimizing the amount of virus particles: Also, the quantity of virus particles, by obvious reasons, plays an important role in the oncolytic virotherapy. This motivates us to introduce another optimal control $u_2(t)$ pertaining to optimize the amount of total free virus particles which are responsible for targeting, infecting and killing tumor cells.

Incorporating these two controls, our aim is to minimize the tumor volume by controlling values of infection rate and viral load. In order to achieve this goal, we, in this section, formulate and study an optimal control problem regarding the delayed oncolytic virotherapy. We introduce these two discussed

optimal control parameters $u_1(t)$ and $u_2(t)$ in our model (2.1). Both the control functions are supposed to be bounded and Lebesgue integrable on the interval $[0, t_f]$, where t_f represents the time during which these controls are to be applied. The optimal control system is given below.

$$\begin{aligned}
\frac{dU}{dt} &= rU(t)\left(1 - \frac{U(t)+I(t)}{K}\right) - \alpha U(t)I(t) - (\beta + u_1(t))U(t)V(t) \\
\frac{dI}{dt} &= (\beta + u_1(t))U(t-\tau)V(t-\tau) - \gamma I(t) \\
\frac{dV}{dt} &= b\gamma I(t) - \delta V(t) - (\beta + u_1(t))U(t)V(t) + u_2(t)V(t).
\end{aligned} \tag{6.1}$$

subjected to the same initial conditions as defined in the system (2.1).

Existence, positivity and boundedness of the solutions can be proved in the same way as we did in the third section. Now, our aim is to minimize the total tumor load while minimizing the efforts of engineering the rate of infection and viral load. Thus, we intend to obtain an optimal infection rate $u_1(t)$ and an optimal viral load $u_2(t)$ so that minimal efforts could result maximum benefits, i.e. the tumor load could be least against the respective cost incurred. Note that the optimal utilization of a resource depends on how a cost function is defined. Thus, based on the above discussion, an objective functional $J(u_1, u_2)$ for fixed duration of control t_f and the corresponding admissible control set Ω for the control variables are given as:

$$J(u_1, u_2) = \int_0^{t_f} (U + I + \frac{1}{2}a_1 u_1^2 + \frac{1}{2}a_2 u_2^2)dt, \tag{6.2}$$

where t_f is the treatment period. The parameters a_1 and a_2 are non-negative and represent the weight constants. The control set Ω is defined as

$$\Omega = \{(u_1(t), u_2(t)) : 0 \le u_1, u_2 \le 1 \text{ are Lebesgue integrable for } t \in [0, t_f]\}.$$

Now, our aim is to find such a pair of bounded and Lebesgue integrable control profiles $u_1^*(t)$ and $u_2^*(t)$ so that the cost functional $J(u_1, u_2)$ is minimum, i.e.,

$$J(u_1^*, u_2^*) = \min_{u_1, u_2 \in \Omega} J(u_1, u_2). \tag{6.3}$$

The cost determination in equation (6.2) is done as:

(i) Cost due to tumor load: The cost incurred due to the total tumor load is

$$\int_0^{t_f} (U(t) + I(t))dt.$$

The term $U(t) + I(t)$ represents the cost due to the tumor burden.

(ii) Cost incurred in engineering the rate of infection: Cost involved in modification of virus's rate of infection is

$$\frac{a_1}{2}\int_0^{t_f} u_1^2(t)dt.$$

(iii) Cost incurred in virotherapy: Virotherapy includes the amount of free virus particles injected into the body or directly to tumor to combat with tumor cells. The cost involved in virotherapy is represented by the term

$$\frac{a_2}{2}\int_0^{t_f} u_2^2(t)dt.$$

6.1. **Existence of an optimal control pair.** As demonstrated in [45, 46], the existence of the optimal control can directly be shown. More precisely, we have the following theorem

Theorem 6.1. *There exists an optimal control pair* $(u_1^*, u_2^*) \in \Omega$ *such that*

$$J(u_1^*, u_2^*) = \min_{u_1, u_2 \in \Omega} J(u_1, u_2), \tag{6.4}$$

Proof. We have to check the following conditions before implying the existence result in [45]:

C1: State and control variables are non-negative.
C2: The control set Ω must be closed and convex.
C3: The RHS of the system 6.1 is bounded by a linear functional involving control and state variables.
C4: The integrand of the objective functional must be convex on Ω.
C5: There exists constants η_1 and η_2 both positive and $k > 1$ such that the integrand $L(U, I, u_1, u_2)$ satisfies

$$L(U, I, u_1, u_2) \geq \eta_1(u_1^2 + u_2^2)^{\frac{k}{2}} - \eta_2$$

To verify these conditions and prove the existence, we use [47, 48]. Both the controls and state variables are non-negative that satisfies condition C_1. C_2 is satisfied as by definition the set Ω is closed and convex as well. Condition C_3 is satisfied as the state system is bilinear in u_1 and u_2. Moreover, the integrand of J, i.e., $U + I + \frac{1}{2}a_1u_1^2 + \frac{1}{2}a_2u_2^2$ is convex on Ω. Also, it is clear that there exists a constant $k > 1$ and two numbers η_1 and η_2 such that $J(u_1, u_2) \geq \eta_1(u_1^2 + u_2^2)^{\frac{k}{2}} - \eta_2$ because of the boundedness of the state variables, which completes the existence of an optimal control pair (u_1^*, u_2^*). □

The Lagrangian and Hamiltonian of this optimal control problem are defined as follows

$$L(U, I, u_1, u_2) = U + I + \frac{1}{2}a_1u_1^2 + \frac{1}{2}a_2u_2^2, \tag{6.5}$$

$$H(U, I, u_1, u_2) = L(U, I, u_1, u_2) + \lambda_1\frac{dU}{dt} + \lambda_2\frac{dI}{dt} + \lambda_3\frac{dV}{dt}, \tag{6.6}$$

where the adjoint variables λ_i, i=1,2,3; (as defined in [46]) are determined by solving the following system

$$\begin{aligned}
\frac{d\lambda_1}{dt} &= -\frac{\partial H}{\partial U} - \chi_{[0,t_f-\tau]}\frac{\partial H}{\partial U_\tau}(t+\tau) \\
\frac{d\lambda_2}{dt} &= -\frac{\partial H}{\partial I} \\
\frac{d\lambda_3}{dt} &= -\frac{\partial H}{\partial V} - \chi_{[0,t_f-\tau]}\frac{\partial H}{\partial V_\tau}(t+\tau).
\end{aligned} \tag{6.7}$$

Solving which we get

$$\begin{aligned}
\frac{d\lambda_1}{dt} &= -1 - \lambda_1[r(1 - \frac{2U+I}{K}) - \alpha I - (\beta + u_1)V] - \lambda_2(t+\tau)\chi_{[0,t_f-\tau]}(t)[(\beta+u_1)V_\tau] + \lambda_3[(\beta+u_1)V] \\
\frac{d\lambda_2}{dt} &= -1 - \lambda_1(-\frac{rU}{K} - \alpha U) - \lambda_2(-\gamma) - \lambda_3(b\gamma) \\
\frac{d\lambda_3}{dt} &= -\lambda_1(-(\beta+u_1)U) - \lambda_3(-\delta + u_2) - \chi_{[0,t_f-\tau]}(t)[\lambda_2(t+\tau)(\beta+u_1)U_\tau]
\end{aligned} \tag{6.8}$$

satisfying the transversality condition $\lambda_i(t_f) = 0$; $i = 1, 2, 3$.

Let $\tilde{U}$, $\tilde{I}$ and $\tilde{V}$ be the optimum values of U, I and V. Let the solution of the system (6.8) be $\tilde{\lambda}_i$; $i = 1, 2, 3$. By using Pontriagin et al. [47] Kamien and Schwartz [46], we state and prove the following theorem.

Theorem 6.2. *The optimal controls u_1^*, $u_2^* \in \Omega$ such that $J(u_1^*, u_2^*) = \min_{u_1,u_2\in\Omega} J(u_1, u_2)$ subjected to the system (6.1) are given by $u_1^* = min\{1, max(0, \tilde{u}_1)\}$ and $u_2^* = min\{1, max(0, \tilde{u}_2)\}$ where $\tilde{u}_1 = \frac{\beta\tilde{U}\tilde{V}(\lambda_1+\lambda_3)-\lambda_2\tilde{U}_\tau\tilde{V}_\tau}{a_1}$ and $\tilde{u}_2 = \frac{-\lambda_3\tilde{V}}{a_2}$.*

Proof. To get the optimal controls, we use the condition of optimality

$$\frac{\partial H}{\partial u_1} = 0, \frac{\partial H}{\partial u_2} = 0,$$

we get

$$u_1 = \frac{\tilde{U}\tilde{V}(\lambda_1 + \lambda_3) - \lambda_2 \tilde{U}_\tau \tilde{V}_\tau}{a_1} = \tilde{u}_1$$

$$u_2 = \frac{-\lambda_3 \tilde{V}}{a_2} = \tilde{u}_2$$

Furthermore, lower and upper bounds for these control are 0 and 1 respectively. i.e. if $\tilde{u}_1 < 0$ and $\tilde{u}_2 < 0$ then $u_1 = u_2 = 0$ and if $\tilde{u}_1 > 1$ and $\tilde{u}_2 > 1$ then $u_1 = u_2 = 1$, otherwise $u_1 = \tilde{u}_1$ and $u_2 = \tilde{u}_2$. Hence u_1^* and u_2^* are the optimal controls for which $J(u_1^*, u_2^*)$ is optimum. □

7. Numerical Simulation of the delayed Optimal Control Problem

In this section, we simulate the delayed oncolytic model 6.1 using two optimal controls. The values of the parameters used in the simulation are the same as taken for simulating the problem without control. The weight constants used in the cost functional are taken as: $a_1 = 100$ and $a_2 = 100$. For solving the problem numerically, we adopt a method namely forward-backward sweep method as described in [38, 46, 49]. Following this method, we first use the forward Euler method in state variables and start with an initial control presumption. Next, we apply backward Euler method to solve the adjoint system using transversality conditions and state variables' solution. We then using the obtained values of state variables and adjoint variables, update the control variables $u_1(t)$ and $u_2(t)$. Repeat the same process as many times as the number of intervals taken of the final time. To explore the effect of control policies on the dynamics of tumor growth we used the following three strategies:

(A) Execution of modification in the rate of infection alone: First, we adopt the Strategy $\mathcal{A}$ of engineering the infection rate of virus. Figure-7 together with Figure-8 show that in the absence of delay and control, after 150 *days* the number of uninfected cells attains value 1.4×10^6 and remains there for the rest of the time. When delay τ is taken as 1.9 *days*, periodic damped oscillations start damping very slowly. Further, when Infection-Rate-Optimal control comes into picture in delayed system, number of uninfected cells comes down to 0.96×10^6 which is minimum among without delay-without control, with delay-without control and with delay-with control systems. A similar kind of behavior can be seen in infected cells' and Virus particles' profile. Finally, we observe that total tumor load attains volume 2.04 mm^3, oscillates damping with very slow speed and reaches its minimum value of 1.48 mm^3 respectively when considered without delay-without control, with delay-without control and with delay-with control systems. Figure-9 shows the control profile for Infection-Rate-Optimal control u_1^*.

(B) Execution of modification in viral load alone: Next, we adopt the strategy to control the load of free virus particles. We compare the values of each type of cells, virus particles and total tumor load in the absence and presence of delay τ and control $u_2(t)$. Figure-10 and Figure-11 show that uninfected and infected cells completely wiped out after one small bump in the presence Viral-Load-control. On the other hand, The free virus particles' after 60 *days* mounts to 5×10^6. We observe that the total tumor load faces a small bump on 22^{nd} *day* which mounts up to 0.65×10^6 and pacifies after 42^{nd} *day* coming down to zero. Figure-12 shows the control profile for Viral-Load-Optimal control u_2^*. This suggests that opting Strategy $\mathcal{B}$ alone is better than opting Strategy $\mathcal{A}$ alone and is much more fruitful in order to eliminate tumor.

(C) Combination of both the Strategies A and $\mathcal{B}$ simultaneously: Finally, we combine both the strategies together, i.e., we opt to engineer the rate of infection and viral load together. In this case, we see that the small bump that was appeared in the profile of uninfected cells, infected cells and hence of total tumor load in Strategy $\mathcal{B}$, is almost negligible here in the combination of both the strategies, see Figure-13 and Figure-14. The total tumor, in this case, extincts after 14 *days* (if we neglect that negligible bump). Figure-15 shows the control profiles for Infection-Rate-Optimal control u_1^* and Viral-Load-Optimal control u_2^*. It suggests that the optimal values of controls should be $u_1^* = 0.048$ after 55 *days* and $u_2^* = 1$ after 20 *days*.

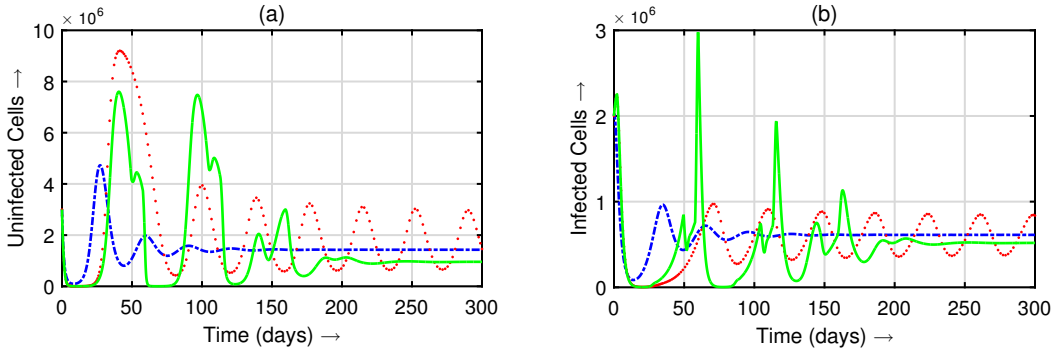

FIGURE 7. Uninfected cells and infected cells profile for without delay-without control (blue dash-dot line), with delay-without control (red dotted line) and with delay-with control (green solid line) under Strategy $\mathcal{A}$.

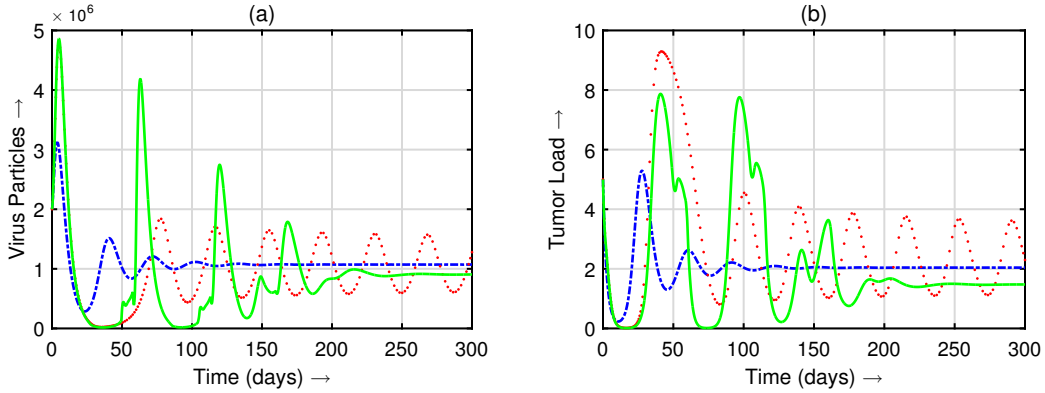

FIGURE 8. Virus particles and total tumor load for without delay-without control (blue dash-dot line), with delay-without control (red dotted line) and with delay-with control (green solid line) under Strategy $\mathcal{A}$.

8. Discussion and Conclusions

In this paper, we have analyzed a three population virus-host delayed dynamical model with optimal control by introducing first, the delay (which is defined as the time taken by an infected cell to become actively infected) and then two optimal controls in the model proposed by A. El-alami laaroussi et al. [24]. At first, we have studied the delayed dynamical system without optimal controls. We checked the stability of all the three steady states after showing the non negativity and boundedness of the solutions and defining the positive bounded feasible region for the analysis of stability of the system. Then, we have shown the direction of stability whose proof is present in the Appendix. The origin or the tumor free steady state is always an unstable state of the system in absence of controls. The instability of origin indicates that the complete eradication of the tumor is not possible in the system without control.

An important parameter in our model is the burst value b which is the number of virus released by the rupture of an infected cell. If $b \leq 1 + \frac{\delta}{\beta K}$, then a stable boundary equilibrium point $E_2(10, 0, 0)$ exists. Furthermore, it is shown that $(10, 0, 0)$ is globally asymptotically stable (Figure-1). Biologically,

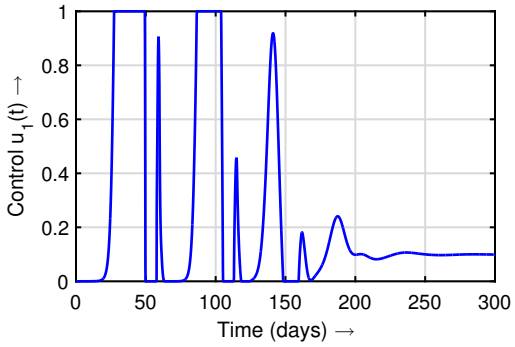

FIGURE 9. Infection-Rate-Optimal control $u_1(t)$ for delayed control problem 6.1 with $\tau = 2$ *days*.

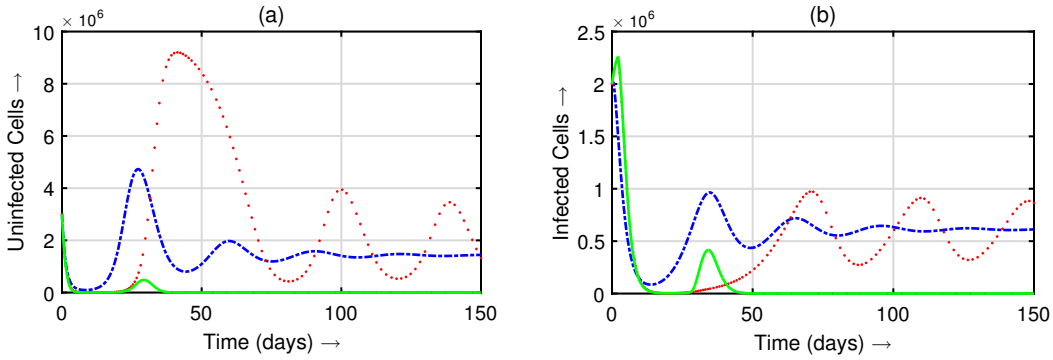

FIGURE 10. Uninfected cells and infected cells profile for without delay-without control (blue dash-dot line), with delay-without control (red dotted line) and with delay-with control (green solid line) under Strategy $\mathcal{A}$.

it shows that whatever be the value of the delay and initial stage of the tumor, if burst rate is lesser than or equal to the factor $1 + \frac{\delta}{\beta K}$, then the uninfected cells will increase rapidly causing the tumor to achieve the carrying capacity 10 mm^3 consisting only uninfected cells whereas infected cells vanish leading to an incurable stage. So it is concluded that if the burst value b is lesser than or equal to the critical value $1 + \frac{\delta}{\beta K}$, then the therapy fails. As the value of b crosses its critical value, the dynamical system bifurcates and the therapy-failure equilibrium point becomes unstable whereas at the same time, a new positive steady state E_3 appears. Thus system undergoes a transcritical bifurcation at $b = 1 + \frac{\delta}{\beta K}$.

Figure 2 shows that when b crosses the critical value and the delay value is zero then under some defining conditions, the positive equilibrium point is stable leading to the partial success of the therapy because in this case, tumor stabilizes to a certain value and remains there for all time. As τ increases, the tumor starts to oscillate finitely weakening the stability of positive equilibrium point. But the tumor remains stable (with enhanced period of becoming stale) for small values of τ. However, if τ crosses its critical value $\tau^* = 2$ *days*, then the corresponding characteristic equation possesses purely imaginary roots showing the existence of periodic solutions, Figure-3. Consequently at $\tau = \tau^*$, the Hopf bifurcation exists and at $\tau > \tau^*$, the system undergoes instability which biologically predicts the periodic growth of the tumor cells. Instability and periodicity of tumor for increasing values of τ is shown in Figure-5.

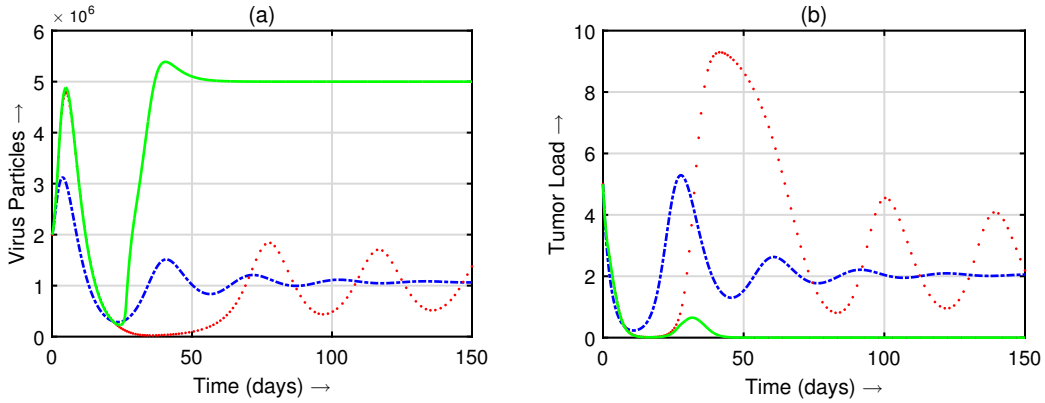

FIGURE 11. Virus particles and total tumor load for without delay-without control (blue dash-dot line), with delay-without control (red dotted line) and with delay-with control (green solid line) under Strategy $\mathcal{B}$.

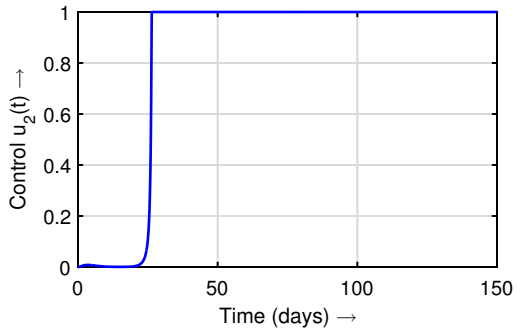

FIGURE 12. Viral-Load-Optimal control $u_2(t)$ for delayed control problem 6.1 with $\tau = 2$ *days*.

Moreover, we have shown in Figure-4 and Figure-6 how the values of β impact over tumor growth. It suggests that if $\beta = 0.02\ mm^{-3}\ day^{-1}$, tumor grows up to its maximal capacity 10 mm^3, if $\beta = 0.22\ mm^{-3}\ day^{-1}$, tumor stabilizes to a certain value 1.9 mm^3 and if $\beta = 0.42\ mm^{-3}\ day^{-1}$, tumor destabilizes again.

At last, we have discussed the delayed optimal control problem under two control policies discussed in Section 6. For, we have adopted three different strategies. Under Strategy $\mathcal{A}$ of engineering the infection rate of virus (Figure-7 and Figure-8), the total tumor load attains the value of 1.48 mm^3, which is lesser than the tumor volume obtained in the delayed system without control. Next, we have adopted the Strategy $\mathcal{B}$ to control the viral load in body. Under this strategy, We observe that the total tumor load gets eliminated after 16 *days* and then experiences a small bump after 22^{nd} *day* reaching its maximum value to 0.65×10^6 and eventually vanishes after 42^{nd} *day*, see Figure-10 and Figure-11. This suggests that opting Strategy $\mathcal{B}$ alone is better than opting Strategy $\mathcal{A}$ alone and is much more fruitful when it comes to eliminating tumor. Finally, we combine both the strategies together, i.e., we decide to engineer the rate of infection and control viral load together. In this case, we see that the total tumor load goes extinct just after 14 *days* and the small bump appeared in Strategy $\mathcal{B}$ is almost disappeared here in the combination of both the strategies, see Figure-13 and Figure-14. Figure-15 shows the control profiles for

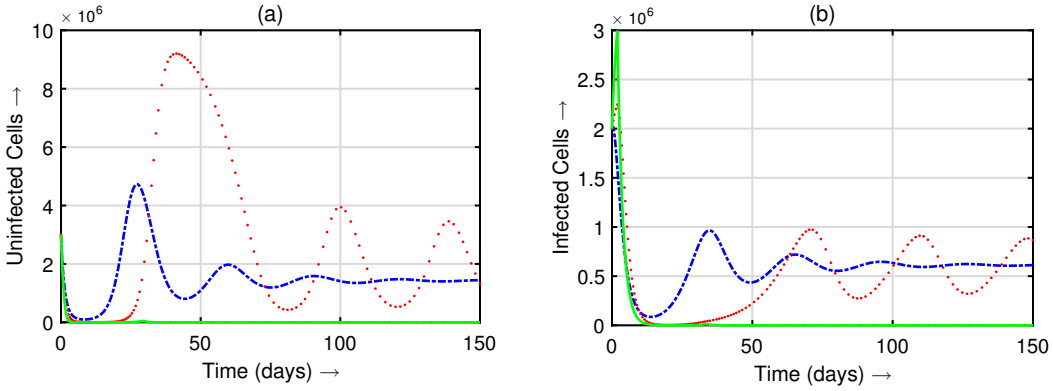

FIGURE 13. Uninfected cells and infected cells profile for without delay-without control (blue dash-dot line), with delay-without control (red dotted line) and with delay-with control (green solid line) under Strategy $\mathcal{A}$.

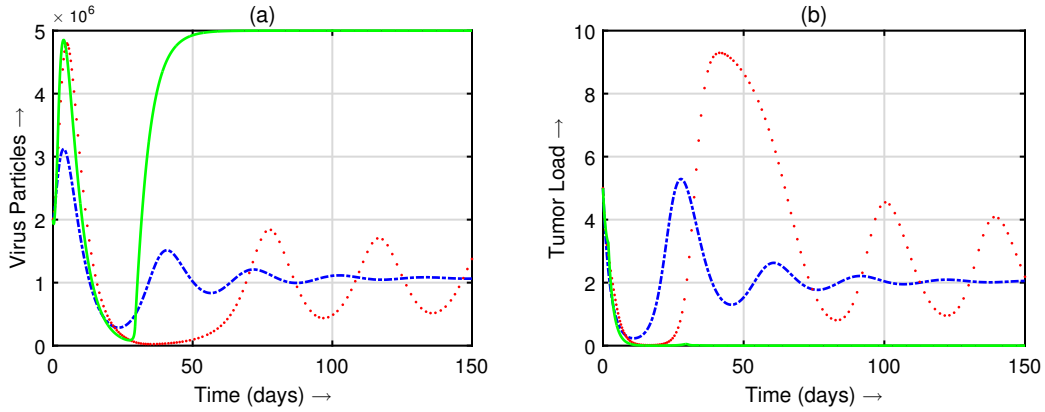

FIGURE 14. Virus particles and total tumor load for without delay-without control (blue dash-dot line), with delay-without control (red dotted line) and with delay-with control (green solid line) under Strategy $\mathcal{B}$.

Infection-Rate-Optimal control u_1^* and Viral-Load-Optimal control u_2^* which suggest that the optimal values of controls are $u_1^* = 0.048$ after 55 *days* and $u_2^* = 1$ after 20 *days*. Thus, we see that when the combination of Strategies $\mathcal{A}$ and $\mathcal{B}$ is applied, extinction of tumor takes place very fast which is never possible in a delayed model without optimal control or in any other strategy alone. Further, we conclude that the results of virotherapy are in this order from worst to best: delayed virotherapy with no optimal control, delayed virotherapy with Strategy $\mathcal{A}$, delayed virotherapy with Strategy $\mathcal{B}$ and delayed virotherapy with Strategies $\mathcal{A}$ and $\mathcal{B}$.

ACKNOWLEDGEMENT AND DECLARATION OF COMPETING INTEREST

The first author of this paper is grateful to the valuable guidance of Dr. Sandip Banerjee, department of mathematics, IIT Roorkee. Further, the research work of the first author is financially supported by the "Council of Scientific and Industrial Research, New Delhi, India". This work does not have any conflicts of interest.

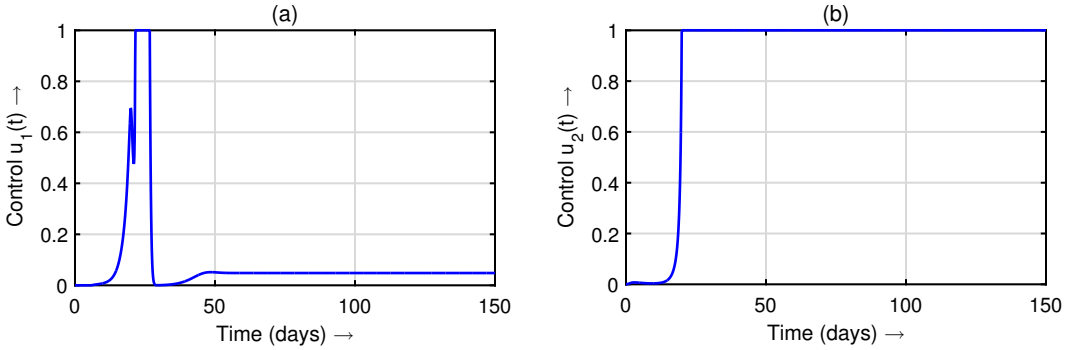

FIGURE 15. Infection-Rate-Optimal control $u_1(t)$ and Viral-Load-Optimal control $u_2(t)$ for delayed control problem 6.1 with $\tau = 2$ *days*.

REFERENCES

[1] Freddie Bray, Ahmedin Jemal, Nathan Grey, Jacques Ferlay, and David Forman. Global cancer transitions according to the human development index (2008–2030): a population-based study. *The lancet oncology*, 13(8):790–801, 2012.

[2] J Ferlay, I Soerjomataram, M Ervik, R Dikshit, S Eser, C Mathers, M Rebelo, DM Parkin, D Forman, and F Bray. Globocan 2012 v1. 0, cancer incidence and mortality worldwide: Iarc cancerbase no. 11. lyon, france: International agency for research on cancer; 2013, 2014.

[3] E Antonio Chiocca. Oncolytic viruses. *Nature Reviews Cancer*, 2(12):938, 2002.

[4] Hideki Kasuya, Shin Takeda, Shuji Nomoto, and Akimasa Nakao. The potential of oncolytic virus therapy for pancreatic cancer. *Cancer Gene Therapy*, 12(9):725, 2005.

[5] Sarah E Frew, Stephen M Sammut, Alysha F Shore, Joshua K Ramjist, Sara Al-Bader, Rahim Rezaie, Abdallah S Daar, and Peter A Singer. Chinese health biotech and the billion-patient market. *Nature Biotechnology*, 26(1):37, 2008.

[6] Ken Garber. China approves world's first oncolytic virus therapy for cancer treatment. *Journal of the National Cancer Institute*, 98(5):298–300, 2006.

[7] David Kirn, Terry Hermiston, and Frank McCormick. Onyx-015: clinical data are encouraging. *Nature medicine*, 4(12):1341, 1998.

[8] Frank McCormick. Cancer specific viruses and the development of onyx-015. *Cancer biology & therapy*, 2(sup1):156–159, 2003.

[9] Douglas D Barker and Arnold J Berk. Adenovirus proteins from both e1b reading frames are required for transformation of rodent cells by viral infection and dna transfection. *Virology*, 156(1):107–121, 1987.

[10] Martin A Nowak and Charles RM Bangham. Population dynamics of immune responses to persistent viruses. *Science*, 272(5258):74–79, 1996.

[11] Christian Jost, Ovide Arino, and Roger Arditi. About deterministic extinction in ratio-dependent predator-prey models. *Bulletin of Mathematical Biology*, 61(1):19–32, 1999.

[12] Martin Nowak and Robert M May. *Virus dynamics: mathematical principles of immunology and virology: mathematical principles of immunology and virology*. Oxford University Press, UK, 2000.

[13] David D Ho, Avidan U Neumann, Alan S Perelson, Wen Chen, John M Leonard, and Martin Markowitz. Rapid turnover of plasma virions and cd4 lymphocytes in hiv-1 infection. *Nature*, 373(6510):123, 1995.

[14] Xiping Wei, Sajal K Ghosh, Maria E Taylor, Victoria A Johnson, Emilio A Emini, Paul Deutsch, Jeffrey D Lifson, Sebastian Bonhoeffer, Martin A Nowak, Beatrice H Hahn, et al. Viral dynamics in human immunodeficiency virus type 1 infection. *Nature*, 373(6510):117, 1995.

[15] Denise Harrison, Harald Sauthoff, Sheila Heitner, Jaishree Jagirdar, William N Rom, and John G Hay. Wild-type adenovirus decreases tumor xenograft growth, but despite viral persistence complete tumor responses are rarely achieved-deletion of the viral e1b-19-kd gene increases the viral oncolytic effect. *Human gene therapy*, 12(10):1323–1332, 2001.

[16] Avner Friedman and Youshan Tao. Analysis of a model of a virus that replicates selectively in tumor cells. *Journal of mathematical biology*, 47(5):391–423, 2003.

[17] Youshan Tao and Qian Guo. The competitive dynamics between tumor cells, a replication-competent virus and an immune response. *Journal of mathematical biology*, 51(1):37–74, 2005.

[18] Lawrence M Wein, Joseph T Wu, and David H Kirn. Validation and analysis of a mathematical model of a replication-competent oncolytic virus for cancer treatment: implications for virus design and delivery. *Cancer research*, 63(6):1317–1324, 2003.

[19] Roger Arditi and Lev R Ginzburg. Coupling in predator-prey dynamics: ratio-dependence. *Journal of theoretical biology*, 139(3):311–326, 1989.

[20] Dominik Wodarz. Viruses as antitumor weapons: defining conditions for tumor remission. *Cancer research*, 61(8):3501–3507, 2001.

[21] Tzy-Wei Hwang and Yang Kuang. Deterministic extinction effect of parasites on host populations. *Journal of mathematical biology*, 46(1):17–30, 2003.

[22] Artem S Novozhilov, Faina S Berezovskaya, Eugene V Koonin, and Georgy P Karev. Mathematical modeling of antitumor virus therapy: Regimes with complete recovery within the framework of deterministic models. *arXiv preprint q-bio/0512022*, 2005.

[23] Dominik Wodarz. Gene therapy for killing p53-negative cancer cells: use of replicating versus nonreplicating agents. *Human gene therapy*, 14(2):153–159, 2003.

[24] A El-alami laaroussi, Elhia Mohamed, M Rachik, EL Habib Benlahmar, and Z Rachik. Analysis of a mathematical model for treatment of cancer with oncolytic virotherapy. *Applied Mathematical Sciences*, 8:929 – 940, 01 2014.

[25] Crawford S Holling. Some characteristics of simple types of predation and parasitism1. *The canadian entomologist*, 91(7):385–398, 1959.

[26] Michel DuPage, Ann F Cheung, Claire Mazumdar, Monte M Winslow, Roderick Bronson, Leah M Schmidt, Denise Crowley, Jianzhu Chen, and Tyler Jacks. Endogenous t cell responses to antigens expressed in lung adenocarcinomas delay malignant tumor progression. *Cancer cell*, 19(1):72–85, 2011.

[27] Claire Joly Condette, Véronique Bach, Camille Mayeur, Jérôme Gay-Quéheillard, and Hafida Khorsi-Cauet. Chlorpyrifos exposure during perinatal period affects intestinal microbiota associated with delay of maturation of digestive tract in rats. *Journal of pediatric gastroenterology and nutrition*, 61(1):30–40, 2015.

[28] Debaldev Jana, Rashmi Agrawal, and Ranjit Kumar Upadhyay. Top-predator interference and gestation delay as determinants of the dynamics of a realistic model food chain. *Chaos, Solitons & Fractals*, 69:50–63, 2014.

[29] Jai Prakash Tripathi, Syed Abbas, and Manoj Thakur. A density dependent delayed predator–prey model with beddington–deangelis type function response incorporating a prey refuge. *Communications in Nonlinear Science and Numerical Simulation*, 22(1-3):427–450, 2015.

[30] A Kumar and PK Srivastava. Delay induced oscillations in a dynamical model for infectious disease. In *Trends in Biomathematics: Modeling, Optimization and Computational Problems*, pages 313–324. Springer, 2018.

[31] Shigui Ruan and Junjie Wei. On the zeros of transcendental functions with applications to stability of delay differential equations with two delays. *Dynamics of Continuous Discrete and Impulsive Systems Series A*, 10:863–874, 2003.

[32] Sunita Gakkhar and Anuraj Singh. Complex dynamics in a prey predator system with multiple delays. *Communications in Nonlinear Science and Numerical Simulation*, 17(2):914–929, 2012.

[33] Tanuja Das and Prashant K Srivastava. Hopf bifurcation and stability switches in an infectious disease model with incubation delay, information, and saturated treatment. *Journal of Applied Mathematics and Computing*, pages 1–25, 2022.

[34] Syed Abbas, Swati Tyagi, Pushpendra Kumar, Vedat Suat Ertürk, and Shaher Momani. Stability and bifurcation analysis of a fractional-order model of cell-to-cell spread of hiv-1 with a discrete time delay. *Mathematical Methods in the Applied Sciences*, 2022.

[35] Yang Kuang. *Delay differential equations: with applications in population dynamics*, volume 191. Academic press, 1993.

[36] Norman MacDonald. *Biological delay systems: linear stability theory*, volume 9. Cambridge University Press, 2008.

[37] K Gopalsamy. Stability and oscillations in delay differential equations of population dynamics. 1992.

[38] Karam Allali, Sanaa Harroudi, and Delfim FM Torres. Analysis and optimal control of an intracellular delayed hiv model with ctl immune response. *Mathematics in Computer Science*, 12(2):111–127, 2018.

[39] Akhil Kumar Srivastav and Mini Ghosh. Modeling and analysis of the symptomatic and asymptomatic infections of swine flu with optimal control. *Modeling Earth Systems and Environment*, 2(4):1–9, 2016.

[40] Anuj Kumar, Prashant K Srivastava, Yueping Dong, and Yasuhiro Takeuchi. Optimal control of infectious disease: Information-induced vaccination and limited treatment. *Physica A: statistical mechanics and its applications*, 542:123196, 2020.

[41] Oliver Ebert, Katsunori Shinozaki, Chryssanthi Kournioti, Man-Seong Park, Adolfo García-Sastre, and Savio LC Woo. Syncytia induction enhances the oncolytic potential of vesicular stomatitis virus in virotherapy for cancer. *Cancer research*, 64(9):3265–3270, 2004.

[42] Jack K Hale and Sjoerd M Verduyn Lunel. *Introduction to functional differential equations*, volume 99. Springer Science & Business Media, 2013.

[43] Hitesh K Singh and Dwijendra N Pandey. Stability analysis of a fractional-order delay dynamical model on oncolytic virotherapy. *Mathematical Methods in the Applied Sciences*, 44(2):1377–1393, 2021.

[44] Joseph La Salle and Solomon Lefschetz. *Stability by Liapunov's direct method*. Academic Press, 1961.

[45] Wendell H Fleming and Raymond W Rishel. *Deterministic and stochastic optimal control*, volume 1. Springer Science & Business Media, 2012.

[46] Morton I Kamien and Nancy Lou Schwartz. *Dynamic optimization: the calculus of variations and optimal control in economics and management*. Courier Corporation, 2012.

[47] Lev Semenovich Pontryagin. The mathematical theory of optimal processes. 1962.

[48] Dahlard L Lukes and LUKES DL. Differential equations: classical to controlled. 1982.

[49] Suzanne Lenhart and John T Workman. *Optimal control applied to biological models*. Chapman and Hall/CRC, 2007.

[50] Brian D Hassard, BD Hassard, Nicholas D Kazarinoff, Y-H Wan, and Y Wah Wan. *Theory and applications of Hopf bifurcation*, volume 41. CUP Archive, 1981.

Appendix

Proof of Theorem 4.6: We have shown in the discussion in Section 4 that at τ^*, the system undergoes Hopf bifurcation at positive equilibrium state. Now, we shall establish the direction and stability of the periodic solutions of the system (2.1) from the positive equilibrium point. In this regard, we use the normal form theory and center manifold theorem as given by Hassard et al. [50]. Denoting the critical value of τ by τ_k and the corresponding purely imaginary roots by $\pm\iota\omega$.
Let $\tau = \tau_k + \mu$, $\mu \in \mathbb{R}$, so that $\mu = 0$ is the Hopf bifurcation value for the system. Let $\mathcal{C}([-1,0],\ \mathbb{R}^3)$ be the space of continuous real valued functions defined from $[-1,0]$ to $\mathbb{R}^3$. Let $y_1(t) = U(t) - U^*$, $y_2(t) = I(t) - I^*$ and $y_3(t) = V(t) - V^*$, and $x_i(t) = y_i(\tau t)$, for $i = 1,2,3,4$. Then the system (2.1) can be expressed as a functional differential equation in $\mathcal{C}$ as given by

$$\frac{dx}{dt} = L_\mu x_t + f(\mu, x_t) \tag{8.1}$$

where $x(t) = (x_1(t), x_2(t), x_3(t))' \in \mathbb{R}^3$, $x_t(\theta) = x(t+\theta)$, $\theta \in [-1,0]$ and $L_\mu : \mathcal{C} \to \mathbb{R}^3$, and $f : \mathbb{R} \times \mathcal{C} \to \mathbb{R}^3$ as defined below

$$L_\mu \phi = (\tau_k + \mu)[A\phi(0) + B\phi(-1)], \tag{8.2}$$

and

$$f(\mu, x_t) = (\tau_k + \mu) \begin{pmatrix} \frac{-r}{K}\phi_1(0)(\phi_1(0) + \phi_2(0)) - \alpha\phi_1(0)\phi_2(0) - \beta\phi_1(0)\phi_3(0) \\ \beta\phi_1(-1)\phi_3(-1) \\ -\beta\phi_1(0)\phi_3(0) \end{pmatrix} \tag{8.3}$$

for $\phi = (\phi_1, \phi_2, \phi_3)' \in \mathcal{C}$, and matrices A and B are as given in (4.1).
By the Riesz representation theorem, there exists a function $\eta(\theta, \mu)$ whose components are of bounded variation for $\theta \in [-1,0]$ such that

$$L_\mu \phi = \int_{-1}^{0} d\eta(\theta, \mu)\phi(\theta). \tag{8.4}$$

We may choose $\eta(\theta, \mu)$ as

$$\eta(\theta, \mu) = (\tau_k + \mu)[A\delta(\theta) - B\delta(\theta + 1)], \tag{8.5}$$

$\delta(\theta)$ being the Dirac delta function.
For $\phi \in \mathcal{C}^1([-1,0], \mathbb{R}^3)$, define

$$A(\mu)\phi = \begin{cases} \frac{d\phi(\theta)}{d\theta}, & \theta \in [-1,0); \\ \int_{-1}^{0} d\eta(s,\mu)\phi(s), & \theta = 0, \end{cases} \tag{8.6}$$

and

$$B(\mu)\phi = \begin{cases} 0 & \theta \in [-1,0); \\ f(\theta,\mu), & \theta = 0. \end{cases} \tag{8.7}$$

Then the system (8.2) can be written as

$$\dot{x_t} = A(\mu)x_t + B(\mu)x_t, \tag{8.8}$$

where $x_t(\theta) = x(t+\theta)$ for $\theta \in [-1,0]$.
For $\psi \in \mathcal{C}^1([-1,0], (\mathbb{R}^3)^*)$, define

$$A^*\psi(s) = \begin{cases} \frac{-d\psi(s)}{ds}, & s \in [-1,0); \\ \int_{-1}^{0} d\eta(t,0)\psi(-t), & s = 0, \end{cases} \tag{8.9}$$

and a bilinear product

$$\langle \psi, \phi \rangle = \bar{\psi}(0).\phi(0) - \int_{\theta=-1}^{0} \int_{\xi=0}^{\theta} \bar{\psi}(\xi - \theta)d\eta(\theta)\phi(\xi)d(\xi), \tag{8.10}$$

where $\eta(\theta) = \eta(\theta, 0)$. Then $A(0)$ and A^* are adjoint operators. Clearly, $\pm\iota\omega_0\tau_k$ are the eigenvalues of A and hence of A^* also. Now, we seek to determine their corresponding eigenvectors for $A(0)$ and A^* both. Let $q(\theta) = (q_1, q_2, q_3)'e^{\iota\omega_0\tau_0\theta}$ be the eigenvector of $A(0)$ w.r.t. the eigenvalue $\iota\omega_0\tau_k$, then

$$A(0)q(\theta) = \iota\omega_0\tau_k q(\theta), \tag{8.11}$$

For $\theta = 0$, we get

$$\tau_k \begin{pmatrix} \iota\omega_0 - r(1 - \frac{2U^*+I^*}{K}) + \alpha I^* + \beta V^* & r\frac{U^*}{K} + \alpha U^* & \beta U^* \\ -\beta V^* e^{\iota\omega_0\tau_k} & \iota\omega_0 + \gamma & -\beta U^* e^{\iota\omega\tau_k} \\ \beta V^* & -b\gamma & \iota\omega_0 + \delta + \beta U^* \end{pmatrix} \begin{pmatrix} q_1 \\ q_2 \\ q_3 \end{pmatrix} = \begin{pmatrix} 0 \\ 0 \\ 0 \end{pmatrix} \tag{8.12}$$

Solving the above system choosing $q_1 = 1$, we get $q_2 = \frac{\beta V^*(\iota\omega_0+\delta)}{e^{-\iota\omega_0\tau_k}[(\gamma+\iota\omega_0)(\delta+\beta U^*+\iota\omega_0)]-b\beta\gamma U^*}$ and $q_3 = \frac{b\beta\gamma V^* - \beta(\iota\omega_0+\gamma)V^* e^{-\iota\omega_0\tau_k}}{e^{-\iota\omega_0\tau_k}[(\gamma+\iota\omega_0)(\delta+\beta U^*+\iota\omega_0)]-b\beta\gamma U^*}$

Similarly, suppose $q^*(s) = D(q_1^*, q_2^*, q_3^*)'e^{\iota\omega_0\tau_0 s}$ be the eigenvector of A^* corresponding to the eigenvalue $-\iota\omega_0\tau_k$, then

$$A^* q^*(s) = -\iota\omega_0\tau_k q^*(s). \tag{8.13}$$

Solving 8.13, we get $q_1^* = 1$, $q_2^* = \frac{U^*(\iota\omega_0-\delta-\beta U^*)(\frac{r}{K}+\alpha)-b\beta\gamma U^*}{(\gamma-\iota\omega_0)(\delta+\beta U^*-\iota\omega_0)-b\beta\gamma U^* e^{-\iota\omega_0\tau_k}}$ and $q_3^* = \frac{-\beta U^{*2} e^{-\iota\omega_0\tau_k}(\frac{r}{K}+\alpha)-\beta U^*(\gamma-\iota\omega_0)}{(\gamma-\iota\omega_0)(\delta+\beta U^*-\iota\omega_0)-b\beta\gamma U^* e^{-\iota\omega_0\tau_k}}$

Using the normalization condition, i.e., $\langle q^*(s)q(\theta)\rangle = 1$, we have from 8.10

$$\begin{aligned}
\langle q^*(s), q(\theta)\rangle &= \bar{D}(1, \bar{q_2^*}, \bar{q_3^*})(1, q_2, q_3)' - \int_{-1}^{0}\int_{\xi=0}^{\theta} \bar{D}(1, \bar{q_2^*}, \bar{q_3^*})e^{-\iota\omega_0\tau_0(\xi-\theta)}d\eta(\theta)(1, q_2, q_3)'e^{\iota\omega_0\tau_0\xi}d\xi, \\
&= \bar{D}[1 + q_2\bar{q_2^*} + q_3\bar{q_3^*} - \int_{-1}^{0}(1, \bar{q_2^*}, \bar{q_3^*})\theta e^{\iota\omega_0\tau_0\theta}d\eta(\theta)(1, q_2, q_3)'], \\
&= \bar{D}[1 + q_2\bar{q_2^*} + q_3\bar{q_3^*} + \tau_0 e^{-\iota\omega_0\tau_0}(1, \bar{q_2^*}, \bar{q_3^*}) \times B(1, q_2, q_3)', \\
&= \beta\bar{q_1^*}(V^* + U^* q_2).
\end{aligned}$$

As given in Hassard et al. [50], we first determine the coordinates to describe the center manifold $\mathcal{C}_0$ at $\mu = 0$. Let x_t be the solution of the equation (8.8) when $\mu = 0$. Define

$$z(t) = \langle q^*, x_t\rangle,\ W(t, \theta) = x_t(\theta) - 2Re\{z(t)q(\theta)\}. \tag{8.14}$$

On the center manifold $\mathcal{C}_0$, we have

$$W(t, \theta) = W(z, \bar{z}, \theta) = W_{20}(\theta)\frac{z^2}{2} + W_{11}(\theta)z\bar{z} + W_{02}(\theta)\frac{\bar{z}^2}{2} + ... \tag{8.15}$$

where z and $\bar{z}$ are local coordinates for the center manifold $\mathcal{C}_0$ in the direction of q^* and $\bar{q^*}$. Note that W is real if x_t is real. We consider only real solutions $x_t \in \mathcal{C}_0$ of the equation (8.8). So

$$\begin{aligned}
\dot{z} &= \iota\omega_0\tau_k z + \bar{q^*}(0)f(0, W(z, \bar{z}, 0) + 2Re\{zq(0)\}), \\
&= \iota\omega_0\tau_k z + g(z, \bar{z}),
\end{aligned} \tag{8.16}$$

where

$$g(z, \bar{z}) = \bar{q^*}(0).f_0(z, \bar{z}) \tag{8.17}$$

$$= g_{20}\frac{z^2}{2} + g_{11}z\bar{z} + g_{02}\frac{\bar{z}^2}{2} + g_{21}\frac{z^2\bar{z}}{2} + ... \tag{8.18}$$

Then, using (8.14) and (8.15), we have

$$x_t(\theta) = W(z, \bar{z}, \theta) + 2Re\{zq(\theta)\}, \tag{8.19}$$

$$= W_{20}(\theta)\frac{z^2}{2} + W_{11}(\theta)z\bar{z} + W_{02}(\theta)\frac{\bar{z}^2}{2} + z(q_1, q_2, q_3)'e^{\iota\omega_0\tau_k\theta} + \bar{z}(\bar{q_1}, \bar{q_2}, \bar{q_3})'e^{-\iota\omega_0\tau_k\theta} + .. \tag{8.20}$$

so that

$$x_t^i(\theta) = W_{20}^{(i)}(\theta)\frac{z^2}{2} + W_{11}^{(i)}(\theta)z\bar{z} + W_{02}^{(i)}(\theta)\frac{\bar{z}^2}{2} + zq_i e^{\iota\omega_0\tau_k\theta} + \bar{z}\bar{q_i}e^{-\iota\omega_0\tau_k\theta}, \tag{8.21}$$

for $i = 1, 2, 3$.
From the equation (8.17), we have

$$g(z,\bar{z}) = \tau_k \bar{D}(\bar{q_1^*}, \bar{q_2^*}, \bar{q_3^*}). \begin{pmatrix} \frac{-r}{K} x_t^1(0)(x_t^1(0) + x_t^2(0)) - \alpha x_t^1(0)x_t^2(0) - \beta x_t^1(0)x_t^3(0) \\ \beta x_t^1(-1)x_t^3(-1) \\ -\beta x_t^1(0)x_t^3(0) \end{pmatrix} \tag{8.22}$$

It is obvious that

$$x_t^1(0) = z + \bar{z} + W_{20}^{(1)}(0)\frac{z^2}{2} + W_{11}^{(1)}(0)z\bar{z} + W_{02}^{(1)}(0)\frac{\bar{z}^2}{2} + ..., \tag{8.23}$$

$$x_t^2(0) = zq_2 + \bar{z}\bar{q_2} + W_{20}^{(2)}(0)\frac{z^2}{2} + W_{11}^{(2)}(0)z\bar{z} + W_{02}^{(2)}(0)\frac{\bar{z}^2}{2} + ..., \tag{8.24}$$

$$x_t^3(0) = zq_3 + \bar{z}\bar{q_3} + W_{20}^{(3)}(0)\frac{z^2}{2} + W_{11}^{(3)}(0)z\bar{z} + W_{02}^{(3)}(0)\frac{\bar{z}^2}{2} + ..., \tag{8.25}$$

$$x_t^1(-1) = W_{20}^{(1)}(-1)\frac{z^2}{2} + W_{11}^{(1)}(-1)z\bar{z} + W_{02}^{(1)}(-1)\frac{\bar{z}^2}{2} + ze^{-\iota\omega_0\tau_k} + \bar{z}e^{\iota\omega_0\tau_k} + ..., \tag{8.26}$$

and

$$x_t^3(-1) = W_{20}^{(3)}(-1)\frac{z^2}{2} + W_{11}^{(3)}(-1)z\bar{z} + W_{02}^{(3)}(-1)\frac{\bar{z}^2}{2} + zq_3e^{-\iota\omega_0\tau_k} + \bar{z}\bar{q_3}e^{\iota\omega_0\tau_k} + ... \tag{8.27}$$

Further,

$$x_t^1(0)x_t^1(0) = z^2 + \bar{z}^2 + 2z\bar{z} + \frac{1}{2}(4W_{11}^{(1)}(0) + 2W_{20}^{(1)}(0))z^2\bar{z} + ..., \tag{8.28}$$

$$x_t^1(0)x_t^2(0) = q_2z^2 + \bar{q_2}\bar{z}^2 + (q_2 + \bar{q_2})z\bar{z} + \frac{1}{2}(2W_{11}^{(2)}(0) + W_{20}^{(2)}(0) + W_{20}^{(1)}(0)\bar{q_2} + 2W_{11}^{(1)}(0)q_2)z^2\bar{z} + ..., \tag{8.29}$$

$$x_t^1(0)x_t^3(0) = q_3z^2 + \bar{q_3}\bar{z}^2 + (q_3 + \bar{q_3})z\bar{z} + \frac{1}{2}(2W_{11}^{(3)}(0) + W_{20}^{(3)}(0) + W_{20}^{(1)}(0)\bar{q_3} + 2W_{11}^{(1)}(0)q_3)z^2\bar{z} + ..., \tag{8.30}$$

and

$$\begin{aligned} x_t^1(-1)x_t^3(-1) = {} & q_3e^{-2\iota\omega_0\tau_k}z^2 + \bar{q_3}e^{2\iota\omega_0\tau_k}\bar{z}^2 + (q_3 + \bar{q_3})z\bar{z} + \frac{1}{2}(2e^{-\iota\omega_0\tau_k}W_{11}^{(3)}(-1) \\ & + e^{\iota\omega_0\tau_k}W_{20}^{(3)}(-1) + \bar{q_3}e^{\iota\omega_0\tau_k}W_{20}^{(1)}(-1) + 2q_3e^{-\iota\omega_0\tau_k}W_{11}^{(1)}(-1))z^2\bar{z} + ... \end{aligned} \tag{8.31}$$

Now, using the values obtained in equations (8.28), (8.29), (8.30) and (8.31) in the equation (8.22), we get,

$$\begin{aligned} g(z,\bar{z}) = {} & \tau_k\bar{D}[(-\frac{r}{K} - \alpha)\{q_2z^2 + \bar{q_2}\bar{z}^2 + (q_2 + \bar{q_2})z\bar{z} + \frac{1}{2}(2W_{11}^{(2)}(0) + W_{20}^{(2)}(0) + W_{20}^{(1)(0)\bar{q_2}} \\ & + 2W_{11}^{(1)}(0))q_2)z^2\bar{z} + ...\} - \frac{r}{K}\{z^2 + \bar{z}^2 + 2z\bar{z} + \frac{1}{2}(4W_{11}^{(1)}(0) + 2W_{20}^{(1)}(0))z^2\bar{z} + ...\} \\ & - \beta\{q_3z^2 + \bar{q_3}\bar{z}^2 + (q_3 + \bar{q_3})z\bar{z} + \frac{1}{2}(2W_{11}^{(3)}(0) + W_{20}^{(3)}(0) + W_{20}^{(1)}(0)\bar{q_3} + 2W_{11}^{(1)}(0)q_3)z^2\bar{z} + ...\} \\ & + \beta\bar{q_2^*}\{q_3e^{-2\iota\omega_0\tau_k}z^2 + \bar{q_3}e^{2\iota\omega_0\tau_k}\bar{z}^2 + (q_3 + \bar{q_3})z\bar{z} + \frac{1}{2}(2e^{-\iota\omega_0\tau_k}W_{11}^{(3)}(-1) + e^{\iota\omega_0\tau_k}W_{20}^{(3)}(-1) \\ & + \bar{q_3}e^{\iota\omega_0\tau_k}W_{20}^{(1)}(-1) + 2q_3e^{-\iota\omega_0\tau_k}W_{11}^{(1)}(-1))z^2\bar{z} + ...\} - \beta\bar{q_3^*}\{q_3z^2 + \bar{q_3}\bar{z}^2 \\ & + (q_3 + \bar{q_3})z\bar{z} + \frac{1}{2}(2W_{11}^{(3)}(0) + W_{20}^{(3)}(0) + \bar{q_3}W_{20}^{(1)}(0) + 2q_3W_{11}^{(1)}(0))z^2\bar{z} + ...\}] \end{aligned}$$

So, comparing the above equation with (8.18), we get

$$g_{20} = 2\tau_k\bar{D}[(-\frac{r}{K} - \alpha)q_2 - \frac{r}{K} - \beta q_3 + \beta\bar{q_2^*}q_3e^{-2\iota\omega_0\tau_k} - \beta\bar{q_3^*}q_3], \tag{8.32}$$

$$g_{02} = 2\tau_k\bar{D}[(-\frac{r}{K} - \alpha)\bar{q_2} - \frac{r}{K} - \beta\bar{q_3} + \beta\bar{q_2^*}\bar{q_3}e^{2\iota\omega_0\tau_k} - \beta\bar{q_3^*}\bar{q_3}], \tag{8.33}$$

$$g_{11} = 2\tau_k\bar{D}[(-\frac{r}{K} - \alpha)(q_2 + \bar{q_2}) - \frac{2r}{K} - \beta(q_3 + \bar{q_3}) + \beta\bar{q_2^*}(q_3 + \bar{q_3})], \tag{8.34}$$

and

$$g_{21} = \tau_k\bar{D}[(-\frac{r}{K}-\alpha)(2W_{11}^{(2)}(0)+W_{20}^{(2)}(0)+W_{20}^{(1)(0)\bar{q}_2}+2W_{11}^{(1)}(0)q_2)-\frac{r}{K}(4W_{11}^{(1)}(0)+2W_{20}^{(1)}(0))$$
$$-\beta(2W_{11}^{(3)}(0)+W_{20}^{(3)}(0)+W_{20}^{(1)}(0)\bar{q}_3+2W_{11}^{(1)}(0)q_3)+\beta\bar{q}_2^*(2e^{-\iota\omega_0\tau_k}W_{11}^{(3)}(-1)+e^{\iota\omega_0\tau_k}W_{20}^{(3)}(-1)$$
$$+\bar{q}_3e^{\iota\omega_0\tau_k}W_{20}^{(1)}(-1)+2q_3e^{-\iota\omega_0\tau_k}W_{11}^{(1)}(-1))-\beta\bar{q}_3^*(2W_{11}^{(3)}(0)+W_{20}^{(3)}(0)+\bar{q}_3W_{20}^{(1)}(0)+2q_3W_{11}^{(1)}(0))]. \tag{8.35}$$

For further evaluation of g_{21}, we require the values of $W_{20}(\theta)$ and $W_{11}(\theta)$. Therefore, from (8.15) and (8.16), we have

$$\begin{aligned}\dot{W} &= \dot{x}_t-\dot{z}q-\dot{\bar{z}}\bar{q}\\ &= \begin{cases} AW-2Re\{\bar{q}^*(0).f_0q(\theta)\}, & \theta\in[-1,0),\\ AW-2Re\{\bar{q}^*(0).f_0q(\theta)\}+f_0, & \theta=0.\end{cases}\\ &= AW+H(z,\bar{z},\theta).\end{aligned} \tag{8.36}$$

where

$$H(z,\bar{z},\theta)=H_{20}(\theta)\frac{z^2}{2}+H_{11}(\theta)z\bar{z}+H_{02}(\theta)\frac{\bar{z}^2}{2}+... \tag{8.37}$$

Also, on the center manifold $\mathcal{C}_0$,

$$\dot{W}=W_z\dot{z}+W_{\bar{z}}\dot{\bar{z}}. \tag{8.38}$$

Using equations (8.16), (8.36) and (8.38), we obtain

$$(A-2\iota\omega_0\tau_k)W_{20} = -H_{20}, \tag{8.39}$$
$$AW_{11} = -H_{11},\ etc. \tag{8.40}$$

Now, for $-1\le\theta<0$,

$$\begin{aligned}H(z,\bar{z},\theta) &= -\bar{q}^*(\theta).f_0q(\theta)-q^*(0).\bar{f}_0\bar{q}(\theta)\\ &= -g(z,\bar{z})q(\theta)-\bar{g}(z,\bar{z})\bar{q}(\theta)\\ &= -(g_{20}q(\theta)+\bar{g}_{02}\bar{q}(\theta))\frac{z^2}{2}-(g_{11}q(\theta)+\bar{g}_{11}\bar{q}(\theta))z\bar{z}+...\end{aligned} \tag{8.41}$$

Comparing the coefficients of above equation with (8.37), we get

$$H_{20}(\theta) = -g_{20}q(\theta)-\bar{g}_{02}\bar{q}(\theta), \tag{8.42}$$
$$H_{11}(\theta) = -g_{11}q(\theta)-\bar{g}_{11}\bar{q}(\theta). \tag{8.43}$$

Using the definition of A and equations (8.39) and (8.42), we get

$$W_{20}'(\theta)=2\iota\omega_0\tau_kW_{20}(\theta)+g_{20}q(\theta)+\bar{g}_{02}\bar{q}(\theta). \tag{8.44}$$

Similarly, from equations (8.40), (8.43) and by definition of A, we have

$$W_{11}'(\theta)=g_{11}q(\theta)+\bar{g}_{11}\bar{q}(\theta), \tag{8.45}$$

Solving the above equations for $W_{20}(\theta)$ and $W_{11}(\theta)$, one can obtain

$$W_{20}(\theta) = \frac{\iota g_{20}}{\omega_0\tau_k}q(0)e^{\iota\omega_0\tau_k\theta}+\frac{\iota\bar{g}_{02}}{3\omega_0\tau_k}\bar{q}(0)e^{-\iota\omega_0\tau_k\theta}+E_1e^{2\iota\omega_0\tau_k\theta}, \tag{8.46}$$
$$W_{11}(\theta) = -\frac{\iota g_{11}}{\omega_0\tau_k}q(0)e^{\iota\omega_0\tau_k\theta}+\frac{\iota\bar{g}_{11}}{\omega_0\tau_k}\bar{q}(0)e^{-\iota\omega_0\tau_k\theta}+E_2. \tag{8.47}$$

where $E_1=(E_1^{(1)},E_1^{(2)},E_1^{(3)})$ and $E_2=(E_2^{(1)},E_2^{(2)},E_2^{(3)})$ are vectors in $\mathbb{R}^3$ and can be obtained by setting $\theta=0$ in $H(z,\bar{z},\theta)$. Further, from the equations (8.39) and (8.40) and using the definition of A, we have

$$\int_{-1}^{0}d\eta(\theta)W_{20}(\theta) = 2\iota\omega_0\tau_kW_{20}-H_{20}(0), \tag{8.48}$$
$$\int_{-1}^{0}d\eta(\theta)W_{11}(\theta) = -H_{11}(0). \tag{8.49}$$

Now, from the equations (8.36), (8.37) and (8.41), we get

$$H_{20}(0) = -g_{20}q(0) - \bar{g}_{02}\bar{q}(0) + \tau_k \begin{pmatrix} -\frac{r}{K} - (\frac{r}{K}+\alpha)q_2 - \beta q_3 \\ \beta q_3 e^{-2\iota\omega_0\tau_k} \\ -\beta q_3 \end{pmatrix}, \tag{8.50}$$

$$H_{11}(0) = -g_{11}q(0) - \bar{g}_{11}\bar{q}(0) + \tau_k \begin{pmatrix} -(\frac{r}{K}+\alpha)(q_2+\bar{q}_2) - \frac{2r}{K} - \beta(q_3+\bar{q}_3) \\ \beta(q_3+\bar{q}_3) \\ -\beta(q_3+\bar{q}_3) \end{pmatrix}. \tag{8.51}$$

Using equations (8.46), (8.48) and (8.50), we get

$$(2\iota\omega_0\tau_k I_3 - \int_{-1}^{0} e^{2\iota\omega_0\tau_k\theta} d\eta(\theta)) = \tau_k \begin{pmatrix} -\frac{r}{K} - (\frac{r}{K}+\alpha)q_2 - \beta q_3 \\ \beta q_3 e^{-2\iota\omega_0\tau_k} \\ -\beta q_3 \end{pmatrix} \tag{8.52}$$

which implies that

$$\begin{pmatrix} 2\iota\omega_0 - r(1-\frac{2U^*+I^*}{K}) + \alpha I^* + \beta V^* & r\frac{U^*}{K} + \alpha U^* & \beta U^* \\ -\beta V^* e^{\iota\omega_0\tau_k} & 2\iota\omega_0 + \gamma & -\beta U^* e^{\iota\omega\tau_k} \\ \beta V^* & -b\gamma & 2\iota\omega_0 + \delta + \beta U^* \end{pmatrix} \begin{pmatrix} E_1^{(1)} \\ E_1^{(2)} \\ E_1^{(3)} \end{pmatrix} = \begin{pmatrix} -\frac{r}{K} - (\frac{r}{K}+\alpha)q_2 - \beta q_3 \\ \beta q_3 e^{-2\iota\omega_0\tau_k} \\ -\beta q_3 \end{pmatrix}. \tag{8.53}$$

Similarly using equations (8.47), (8.49) and (8.51), we get

$$\begin{pmatrix} -r(1-\frac{2U^*+I^*}{K}) + \alpha I^* + \beta V^* & r\frac{U^*}{K} + \alpha U^* & \beta U^* \\ -\beta V^* e^{\iota\omega_0\tau_k} & \gamma & -\beta U^* e^{\iota\omega\tau_k} \\ \beta V^* & -b\gamma & \delta + \beta U^* \end{pmatrix} \begin{pmatrix} E_2^{(1)} \\ E_2^{(2)} \\ E_2^{(3)} \end{pmatrix} = \begin{pmatrix} -(\frac{r}{K}+\alpha)(q_2+\bar{q}_2) - \frac{2r}{K} - \beta(q_3+\bar{q}_3) \\ \beta(q_3+\bar{q}_3) \\ -\beta(q_3+\bar{q}_3) \end{pmatrix}. \tag{8.54}$$

Now, solving the above two systems, we can easily find out the vectors E_1 and E_2 and then W_{20} and W_{11} and hence g_{21}.
Also, we can derive the following parameters as given in Hassard et al. [50].

$$\begin{aligned} c_1(0) &= \frac{\iota}{2\omega_0\tau_k}(g_{11}g_{20} - 2|g_{11}|^2 - \frac{|g_{02}|^3}{2}) + \frac{g_{21}}{2}, \\ \mu_2 &= -\frac{Re\{c_1(0)\}}{Re\{\lambda'(\tau_k)\}}, \\ \beta_2 &= 2Re\{c_1(0)\}, \\ T_2 &= -\frac{Im\{c_1(0)\} + \mu_2 Im\{\lambda'(\tau_k)\}}{\omega_0\tau_k}, \end{aligned}$$

that determine the direction and stability of the periodic solutions from the infected equilibrium at the threshold value $\tau = \tau_k$. This completes the proof.